Refraction index

refractive index $\mu=1-\delta-i\beta$

$$\delta=(e^2\lambda^2/2\pi mc^2)|N+\Sigma_H N_H[\lambda/\lambda_H]^2\ln[\lambda_H^2/\lambda^2-1]|$$

δ (unit decrement) related to the speed in the medium

β related to the absorption

N=electron density (10^{23}-10^{24} el./cm^3)
λ_H=adsorption edge's wavelength

λ far from $\lambda_H \Rightarrow \delta=Ne^2\lambda^2/2\pi mc^2$

$\beta=\lambda\mu_l/4\pi$ μ_l=linear absorption coefficient

the abdus salam
international centre for theoretical physics

elettra

HXR lens

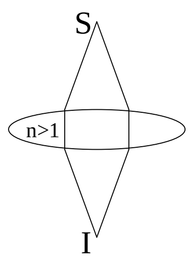

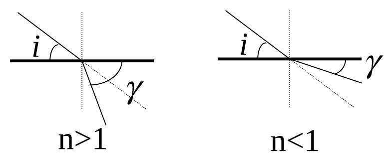

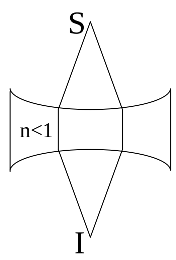

Fermat's principle

$$\frac{1}{f} = (n-1)\left(\frac{1}{R_1}+\frac{1}{R_2}\right) \approx (1-\delta-1)\cdot\frac{2}{R} < 0$$

$$\delta = \frac{Ne^2\lambda^2}{2\pi mc^2} \approx 10^{-2} - 10^{-4}$$

$$\delta \approx 10^{-4} \quad HXR \Rightarrow f \approx 1m \quad if \quad R \approx 1mm$$

HXR berillium lens

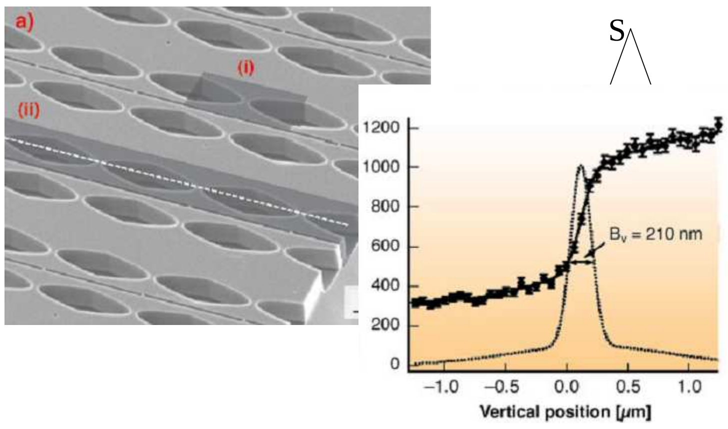

$$\delta \approx 10^{-4} \quad HXR \Rightarrow f \approx 1m \quad if \quad R \approx 1mm$$

Refraction index

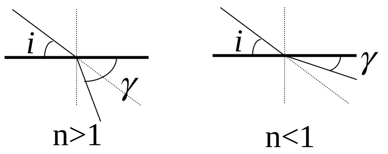

Snell's law: $\cos\gamma = \cos i / n$

$\gamma = 0 \quad n = \cos i_c$

i_c critical angle: total external reflection

$\sin i_c = \lambda (e^2 N / \pi m c^2)^{1/2}$

$\lambda_c(\min) = 3.333 \cdot 10^{-13}\, N^{-1/2} \sin i_c$

Material	Density (g/cm^3)	N (electron/cm^3)	λ_{min} nm
Pentadecane (oil)	0.77	7×10^{22}	64.1sin*i*
Glass	2.6	78×10^{22}	37.9sin*i*
Aluminum oxide	3.9	115×10^{22}	31.2sin*i*
Gold	19.3	466×10^{22}	15.4sin*i*

$i = 5^o$: λ_{min}glass=3.3nm=375 eV
λ_{min}gold=1.34nm=923eV

shorter wavelength needs smaller angles of incidence

Materials with higher density (i.e. higher atomic weight) have higher reflectivity

Mirror reflectivity

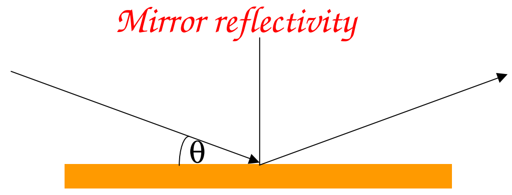

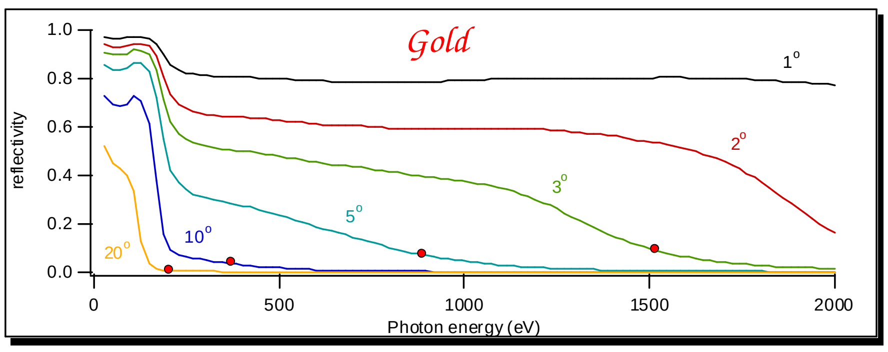

the abdus salam international centre for theoretical physics
elettra

Mirror reflectivity

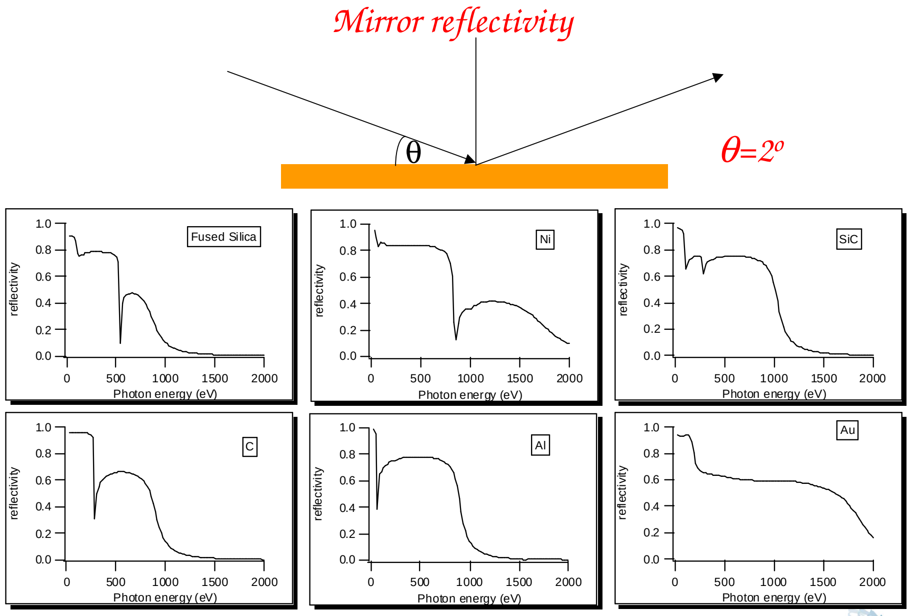

the abdus salam
international centre for theoretical physics

elettra

Figure errors

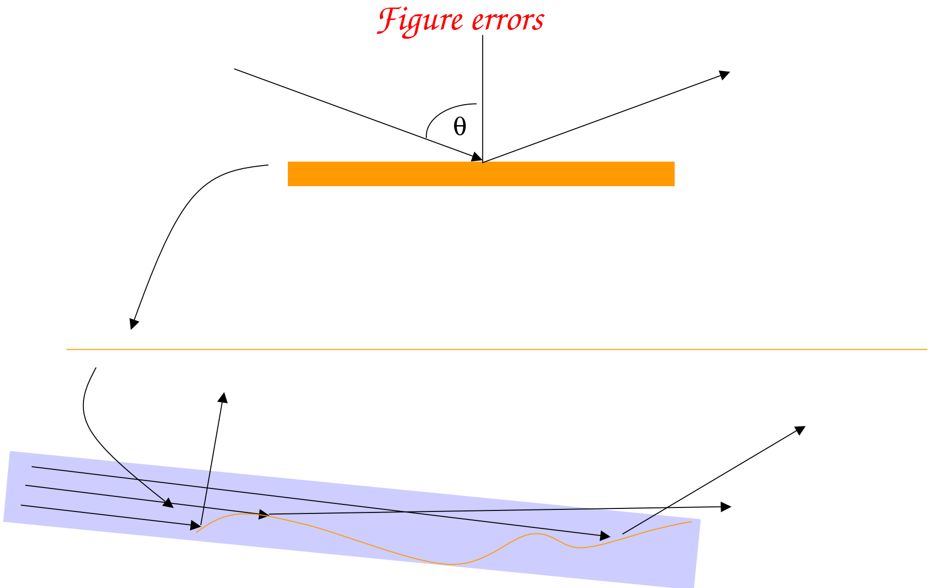

the abdus salam
international centre for theoretical physics

elettra

Figure errors

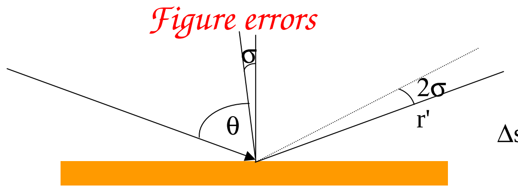

$\Delta s' = 2\, r'\sigma$

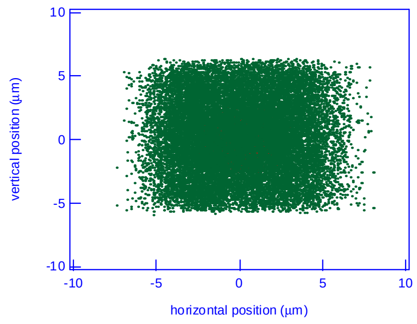

$s' = \sqrt{(Ms)^2 + (2\, r'\sigma)^2}$

Figure errors

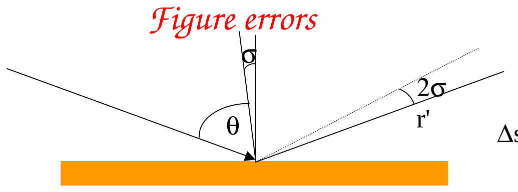

$\Delta s' = 2\, r'\sigma$

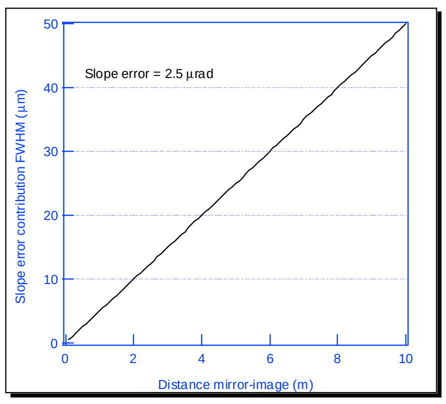

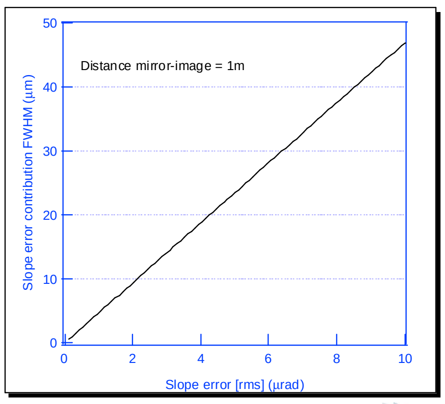

Slope errors (tangential)

Typical manufacturer capabilities *(SESO, ZEISS, Winlight, Jobin Yvon)*

Shape	Length	rms errors
Spherical/flat	Up to 500 mm	< 0.5 µrad
Spherical/flat	> 500 mm	1-2 µrad
Toroidal	Up to 500 mm	< 1 µrad
Toroidal	> 500 mm	> 1 µrad
Aspherical	Up to 500 mm	2 µrad
Aspherical	> 500 mm	3-5 µrad

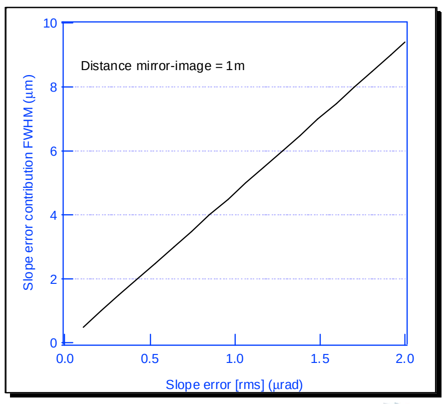

the abdus salam international centre for theoretical physics

elettra

Focal property

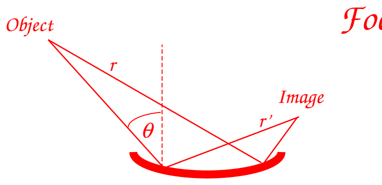

Tangential focusing

Term F_{20} of the optical path function

$(1/r+1/r')\cos\theta/2=1/R$ spherical mirror

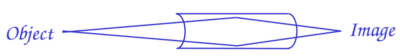

Sagital focusing

Term F_{02} of the optical path function

$(1/r+1/r')/(2\cos\theta)=1/R$ cylindrical/toroidal mirror

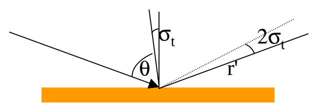

$\Delta s'_t=2\,r'\sigma_t$

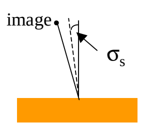

$\Delta s'_s=2\,r'\cos\theta\,\sigma_s$

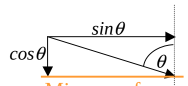

the abdus salam international centre for theoretical physics

elettra

Slope error effect

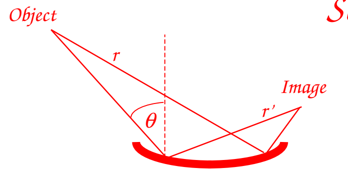

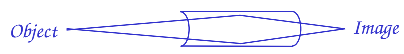

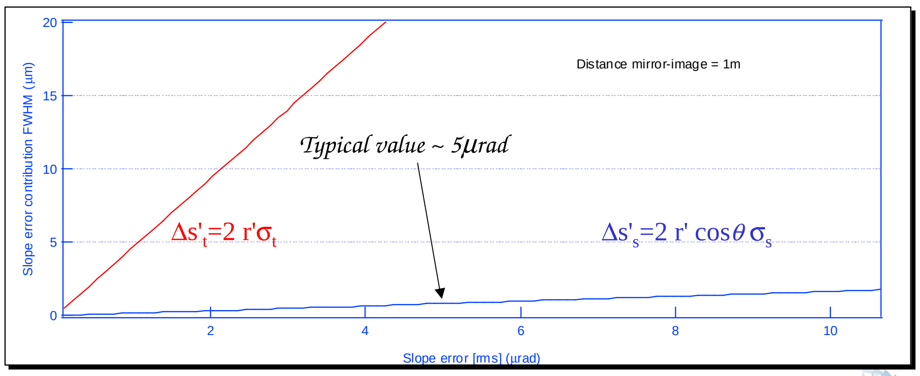

Final focus (F30-F03-F12 …..)

source 80 µm vertical; r=4000 mm r´=400 mm (10:1) θ=88°

Beam divergence 100X100 µrad

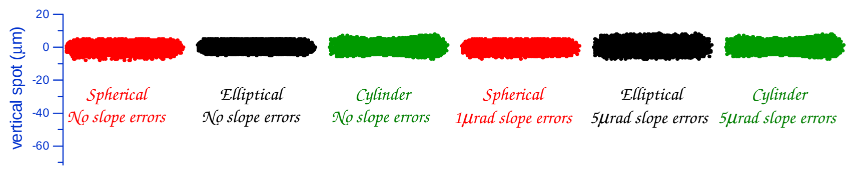

Beam divergence 500X500 µrad

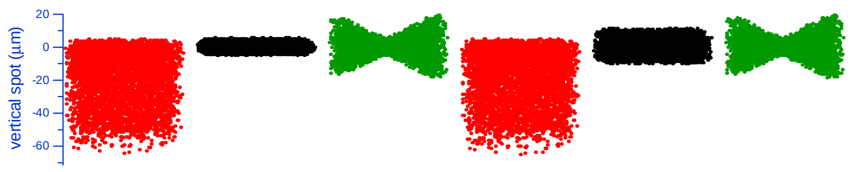

Mirror defects

Slope errors = every deviation from the ideal surface with period larger then ~ 1,2 mm

Typical definition is μrad or arcsec rms.
Alternative definition is λ/10 or λ/20 and so on… P-V or rms
used for normal incidence mirror or "poorer" quality mirrors

Roughness = every deviation from the ideal surface with period smaller then ~ 0.5-1 mm

Typical definition is Å rms.
Alternative definition is surface quality 20-10 or 10-5 (scratch-dig)
used for normal incidence mirror or "poorer" quality mirrors
A dig is nearly equal in terms of its length and width. A scratch could be much longer then width
20-10 means 20/1000 of mm max scratch width 10/100 mm max dig dimension

Roughness

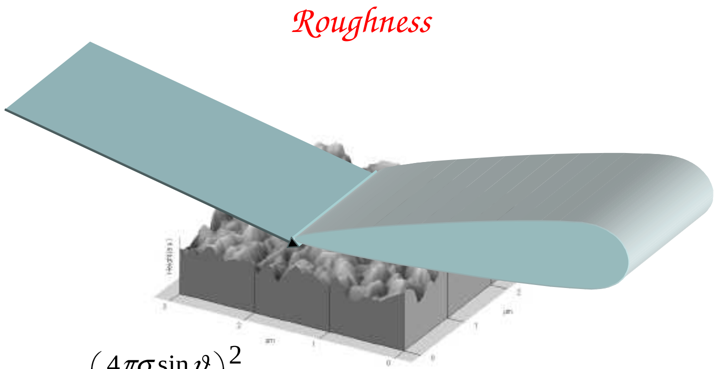

$$I = I_0 e^{-\left(\frac{4\pi\sigma\sin\vartheta}{\lambda}\right)^2}$$

$$\sigma = \sqrt{\frac{1}{n}\sum_{x=0}^{n}\left[s(x) - \overline{s(x)}\right]^2}$$

the abdus salam international centre for theoretical physics
elettra

Power spectral density

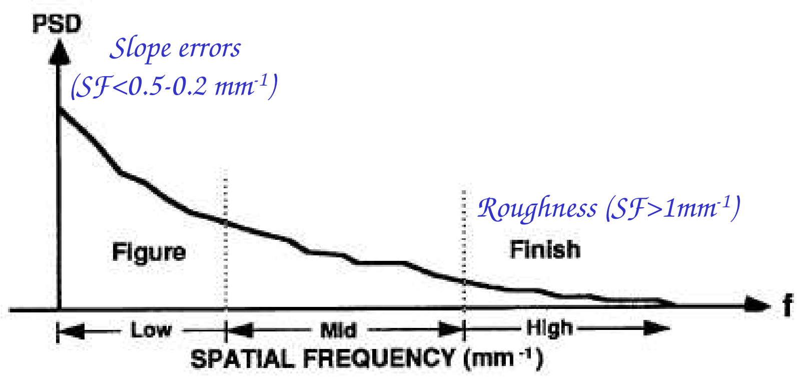

Power spectral density

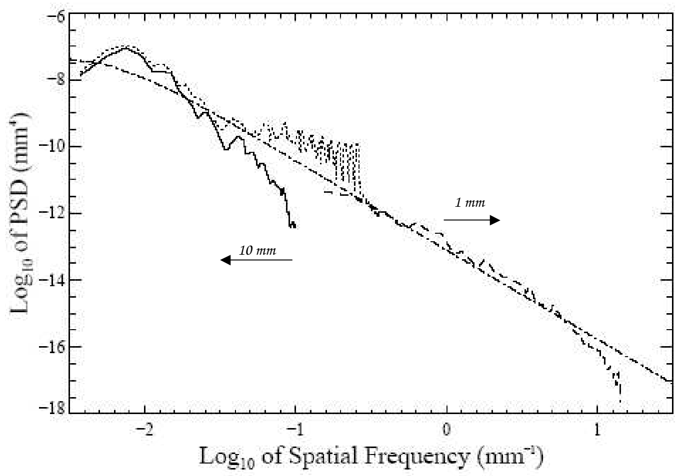

Roughness

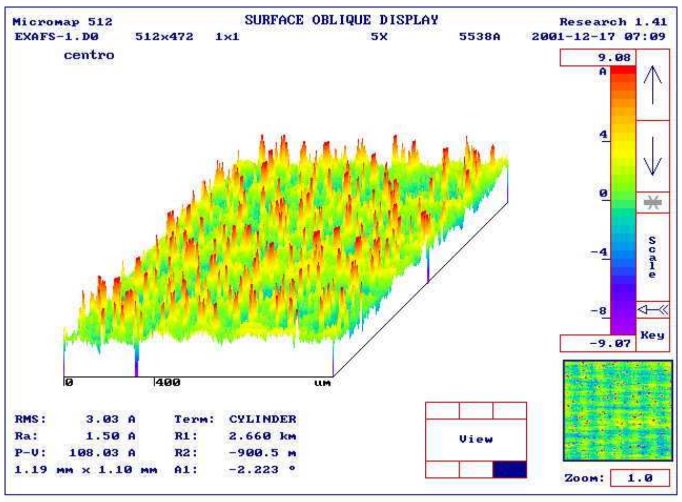

Roughness

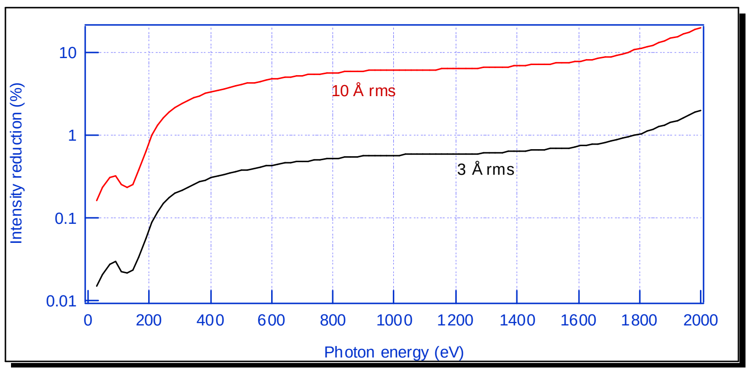

Shape	Spherical/Flat	Toroidal/aspherical
Roughness (Å)	3 standard 1 best	5 standard 3 best

the abdus salam
international centre for theoretical physics

Beamline layout

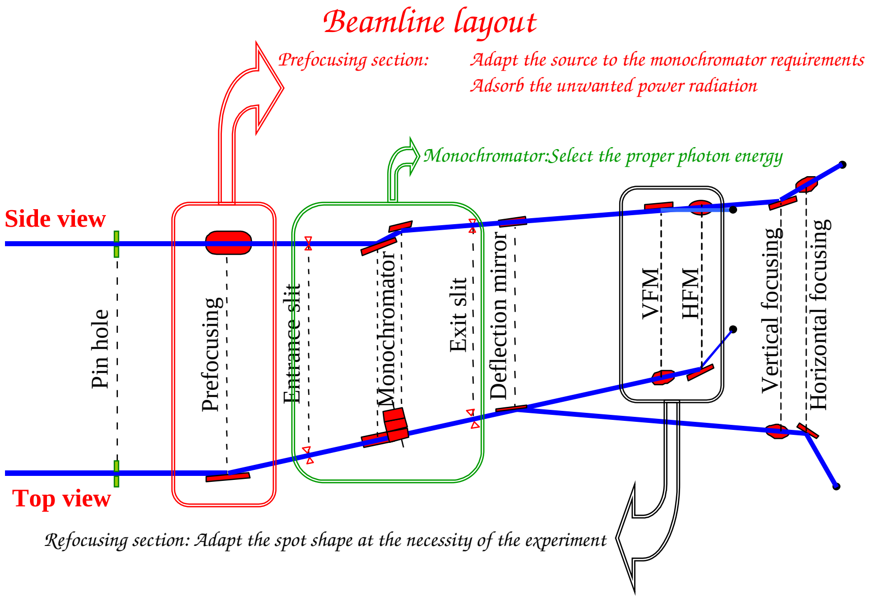

Basic lattice structure

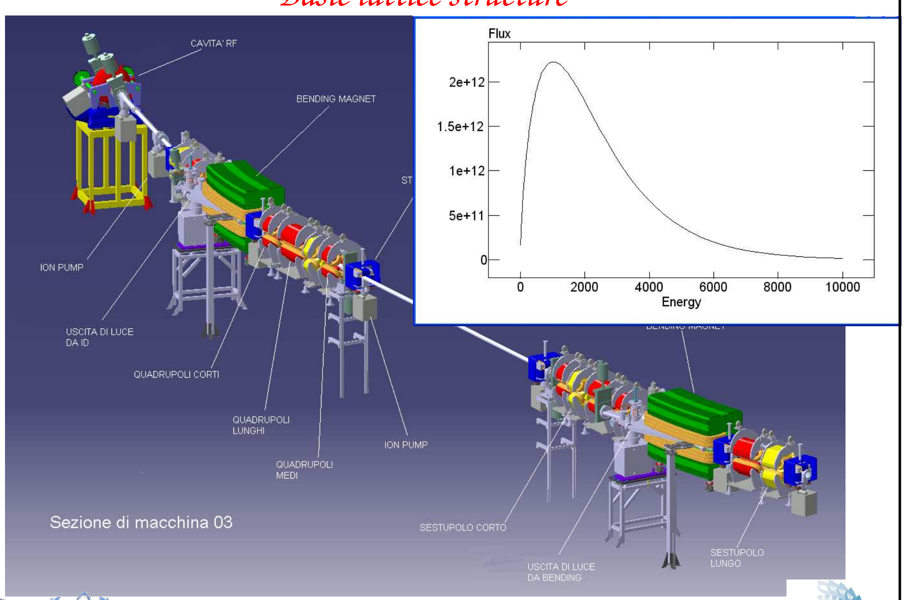

Basic lattice structure

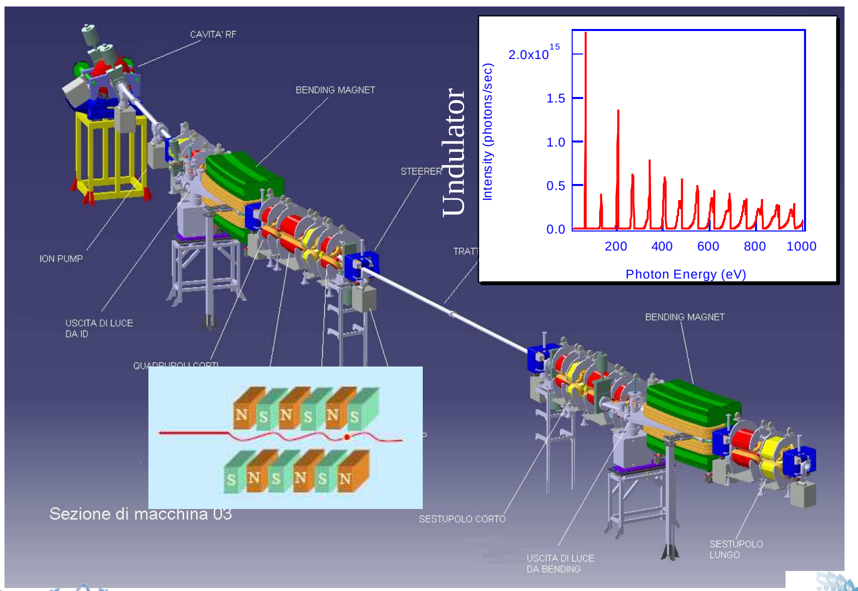

Basic lattice structure

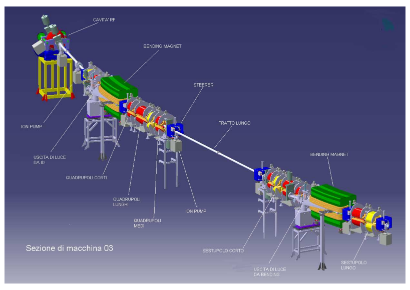

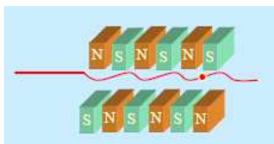

$$\lambda \propto \frac{\lambda_u B^2}{E^2}$$

$$\frac{\Delta\lambda}{\lambda} \propto \frac{1}{nN} \geq \frac{1}{n(80)}$$

$$\sigma \propto \frac{1}{L^{1/2}}$$

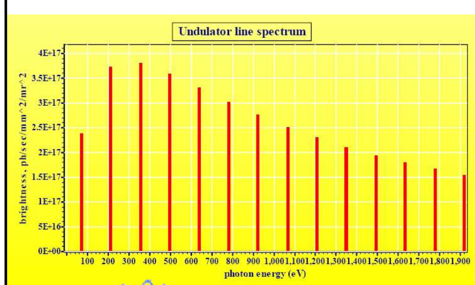

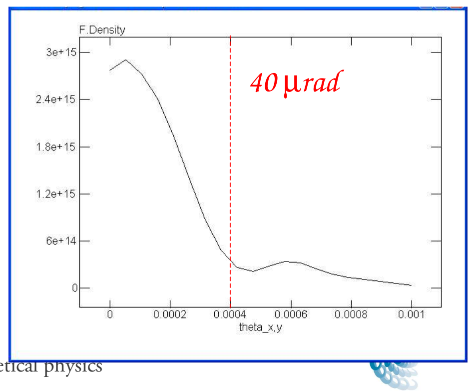

Sources

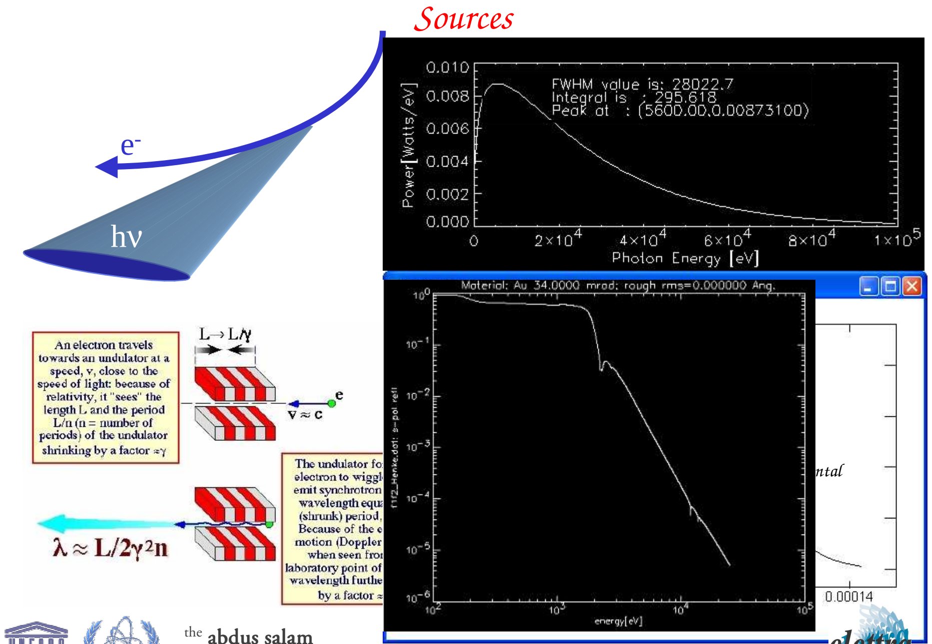

Thermal deformation

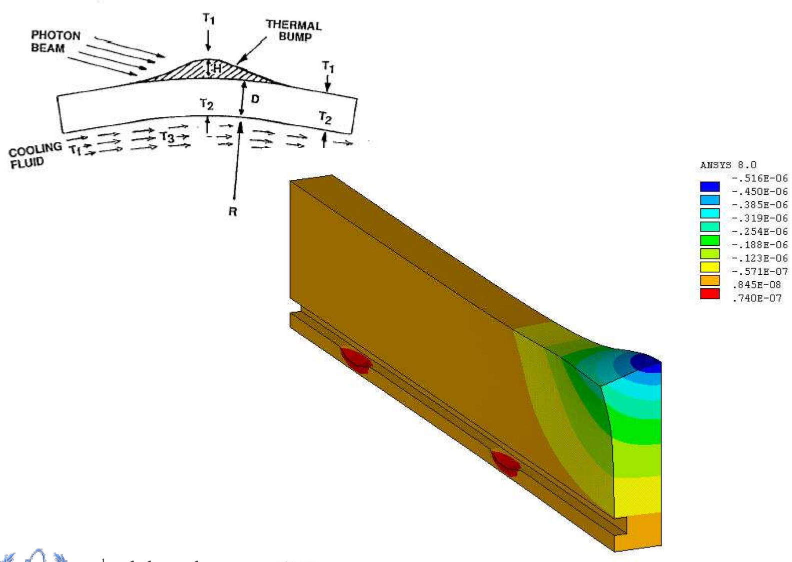

Mechanical and thermal properties of some mirror materials

	Density gm/cc	Young's modulus GPa	Thermal expansion (α) ppm/°C	Thermal conductivity (k) W/m/°C	Figure of merit k/α
Fused silica	2.19	73	0.50	1.4	2.8
Zerodur	2.53	92	0.05	1.60	32
Silicon	2.33	131	2.60	156	60
SiC CVD	3.21	461	2.40	198	82
Aluminum	2.70	68	22.5	167	7.42
Copper	8.94	117	16.5	391	23.7
Glidcop	8.84	130	16.6	365	22
Molybdenum	10.22	324.8	4.80	142	29.6

Silicon mirrors

the abdus salam
international centre for theoretical physics

Side cooling

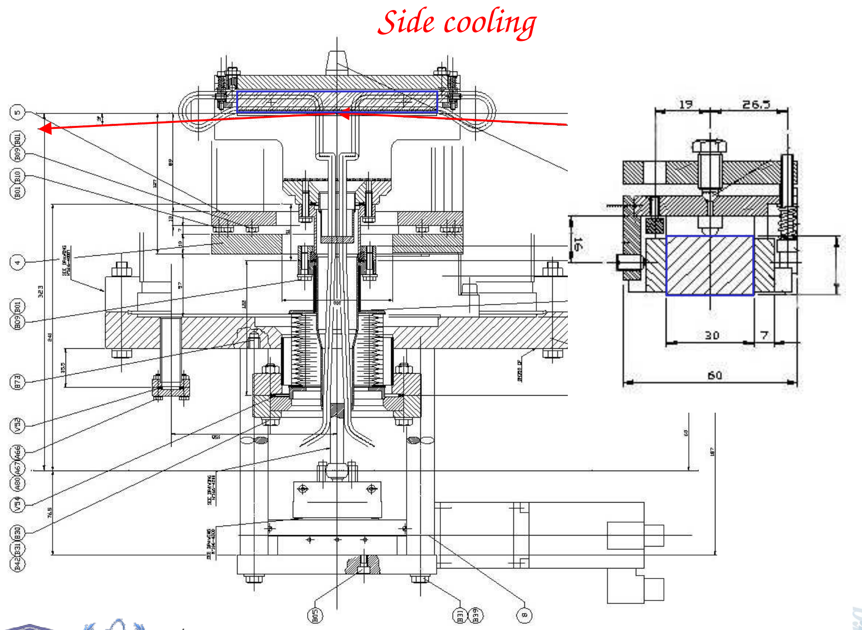

the abdus salam
international centre for theoretical physics

Side cooling

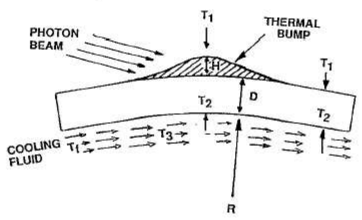

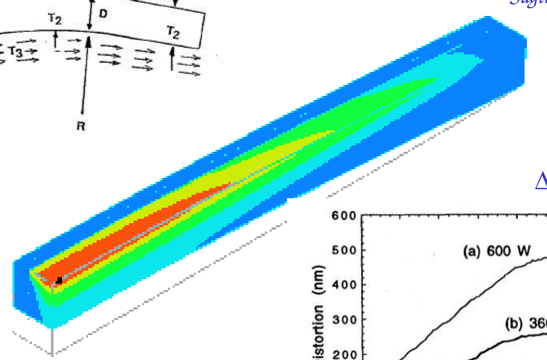

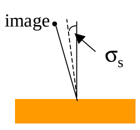

$\Delta s'_s = 2\, r' \cos\theta\, \sigma_s$

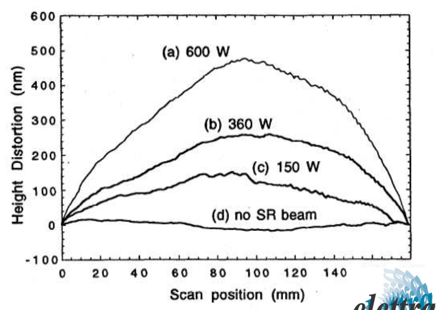

Internal cooling mirror

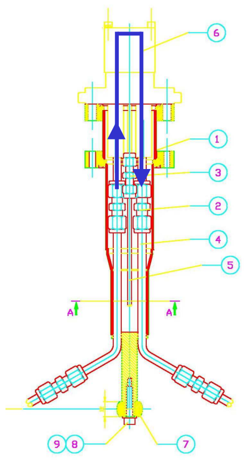

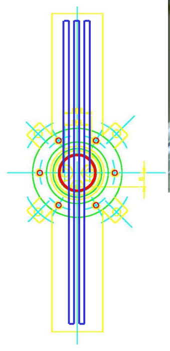

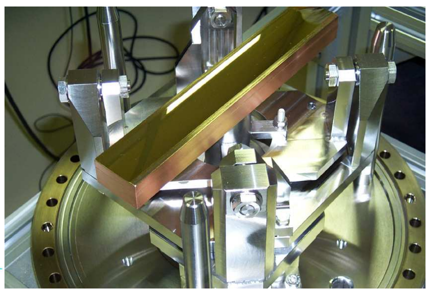

Internal cooling mirror

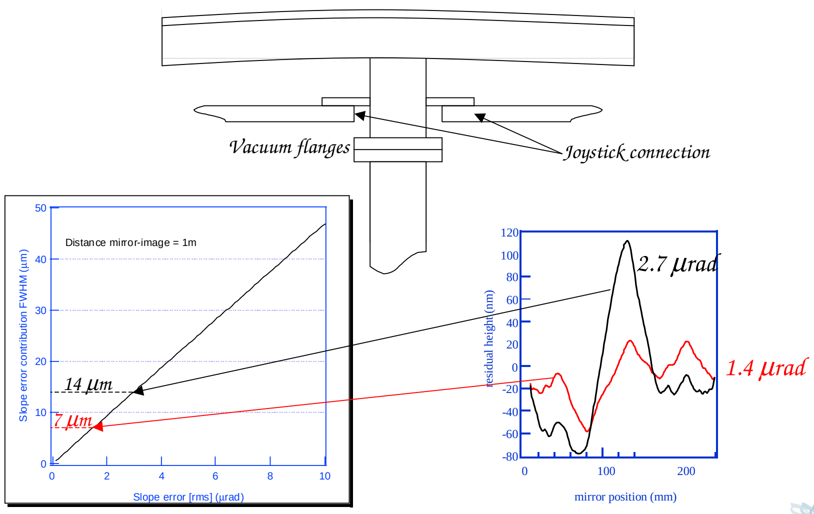

the abdus salam
international centre for theoretical physics

Induced slope errors for 400 W source

glidcop

3GeV Synchrotron source
6.6 cm period undulator K_{max}=5.7
BL6.1

1.5° grazing incidence

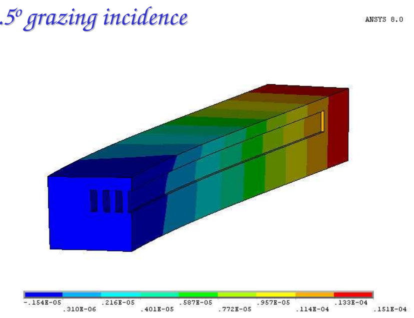

Δh=17μm slope 26 μrad

1.5° grazing incidence

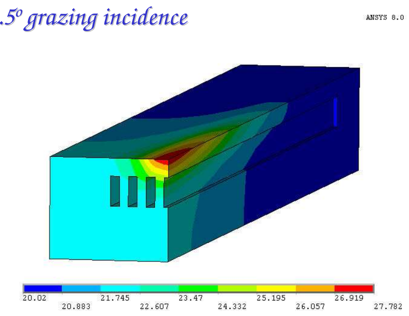

ΔT=7.7°

Induced slope errors for 400 W source

	Density gm/cc	Young's modulus GPa	Thermal expansion (α) ppm/°C	Thermal conductivity (k) W/m/°C	Figure of merit k/α
Silicon	**2.33**	**131**	**2.60**	**156**	**60**
SiC CVD	**3.21**	**461**	**2.40**	**198**	**82**
Aluminum	**2.70**	**68**	**22.5**	**167**	**7.42**
Copper	**8.94**	**117**	**16.5**	**391**	**23.7**
Glidcop	**8.84**	**130**	**16.6**	**365**	**22**
Molybdenum	**10.22**	**324.8**	**4.80**	**142**	**29.6**
I					
S					

Glidcop

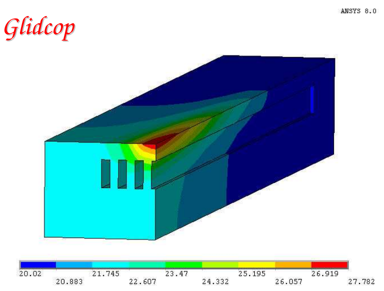

ΔT=7.7°

Molybdenum

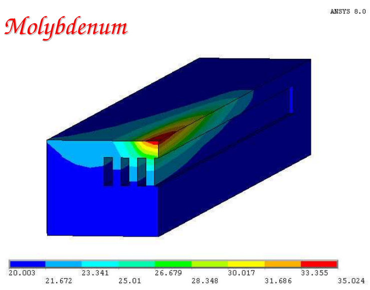

ΔT=13.3°

Induced slope errors for 400 W source

	Density gm/cc	Young's modulus GPa	Thermal expansion (α) ppm/°C	Thermal conductivity (k) W/m/°C	Figure of merit k/α
Silicon	2.33	131	2.60	156	60
SiC CVD	3.21	461	2.40	198	82
Aluminum	2.70	68	22.5	167	7.42
Copper	8.94	117	16.5	391	23.7
Glidcop	8.84	130	16.6	365	22
Molybdenum	10.22	324.8	4.80	142	29.6

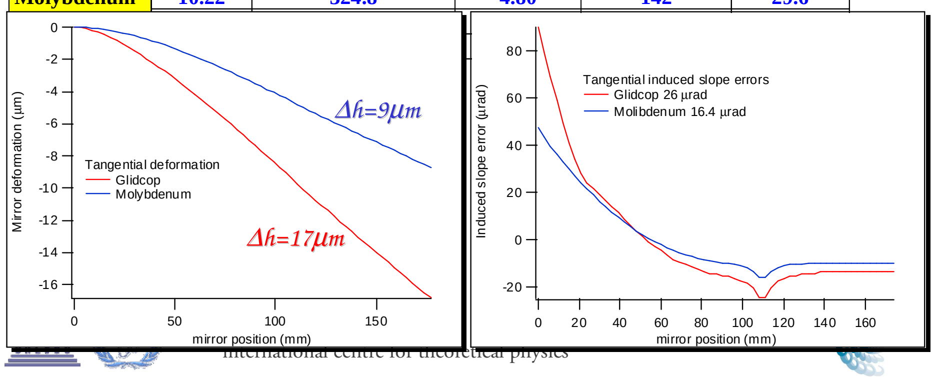

Induced slope errors for 400 W source

	Density gm/cc	Young's modulus GPa	Thermal expansion (α) ppm/°C	Thermal conductivity (k) W/m/°C	Figure of merit k/α
Silicon	2.33	131	2.60	156	60
SiC CVD	3.21	461	2.40	198	82
Aluminum	2.70	68	22.5	167	7.42
Copper	8.94	117	16.5	391	23.7
Glidcop	8.84	130	16.6	365	22
Molybdenum	10.22	324.8	4.80	142	29.6
Invar 36	9.05	141	0.5	10.4	20.8
SuperInvar	8.13	145	0.06	10.5	210

INVAR®
Carpenter Technology Inc.
Alloy 36 iron-nickel(36%) alloy with carbon (0.02%), manganese (0.35%), Silicon (0.2%)
Supernvar: iron-nickel(32%) alloy with carbon (0.02%), manganese (0.40%), Silicon (0.25%), Cobalt (5.5%)

Induced slope errors for 400 W source

	Density gm/cc	Young's modulus GPa	Thermal expansion (α) ppm/°C	Thermal conductivity (k) W/m/°C	Figure of merit k/α
Glidcop	**8.84**	**130**	**16.6**	**365**	**22**
Molybdenum	**10.22**	**324.8**	**4.80**	**142**	**29.6**
SuperInvar	**8.13**	**145**	**0.06**	**10.5**	**210**

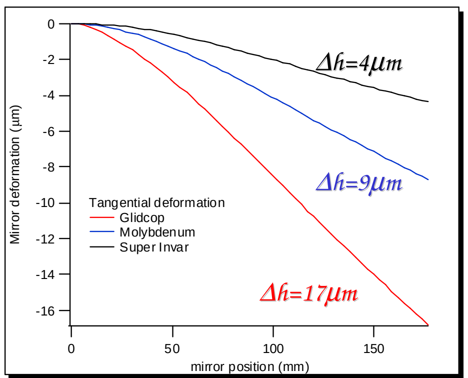

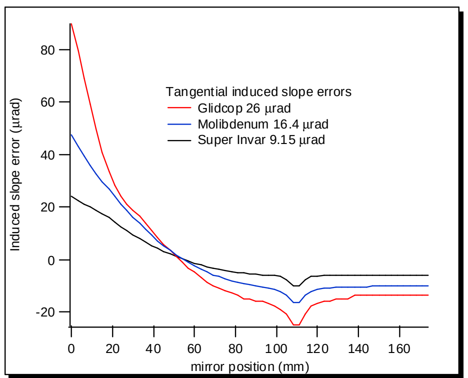

SuperInvar

	Density gm/cc	Young's modulus GPa	Thermal expansion (α) ppm/°C	Thermal conductivity (k) W/m/°C	Figure of merit k/α
Glidcop	**8.84**	**130**	**16.6**	**365**	**22**
Molybdenum	**10.22**	**324.8**	**4.80**	**142**	**29.6**
SuperInvar	**8.13**	**145**	**0.06**	**10.5**	**210**

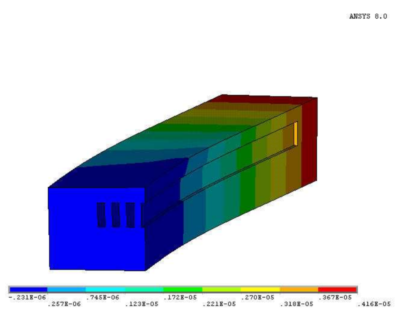

Δh=6μm

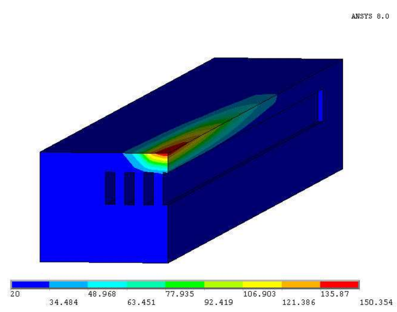

ΔT=130°

Carbon contamination

Effect of the contamination:

- *Strong adsorption at the carbon edge (≈270 eV)*
- *Reduction of reflectivity due to enanchment of the surface roughness*
- *general deterioration of the surface*

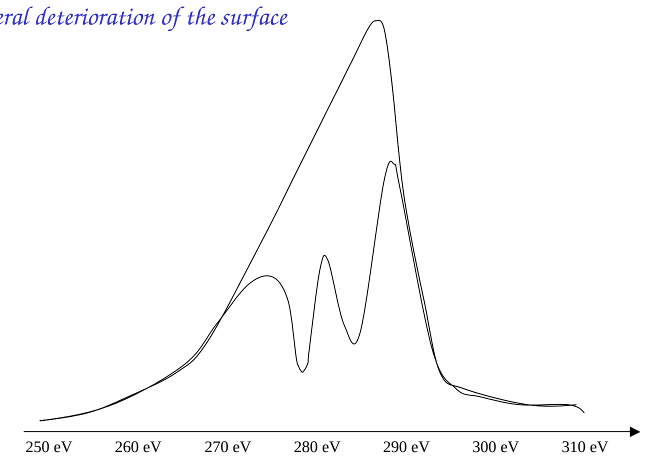

the abdus salam
international centre for theoretical physics

elettra

Carbon contamination and cleaning

Contamination process:

- *Hydrocarbons adsorbed by the surface*
- *Cracking induced by the incoming radiation*
- *Formation of graphitic carbon layer (mixed C coumpond)*

Effect of the contamination:

- *Strong adsorption at the carbon edge (≈270 eV)*
- *Reduction of reflectivity due to enanchment of the surface roughness*
- *general deterioration of the surface*

UV lamp discharge

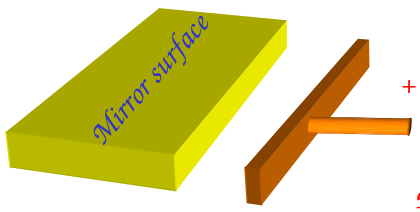

+ 300-500 V (DC)

I 100 mA-1A

P 0.5-1 mbar O_2

the abdus salam
international centre for theoretical physics

elettra

Other contamination

Effect of the contamination:

Strong adsorption at the O/Cr edge

Reduction of reflectivity due to enanchment of the surface roughness

general deterioration of the surface

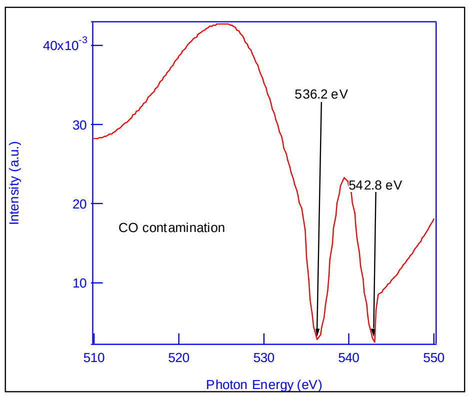

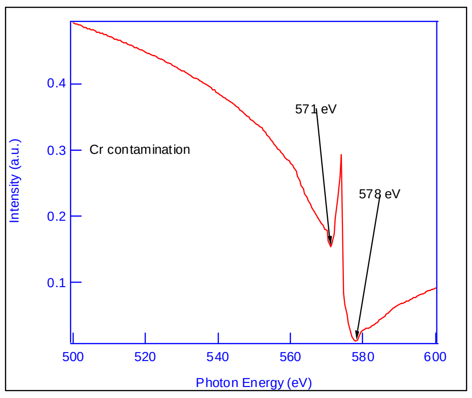

Soft X-ray monochromators

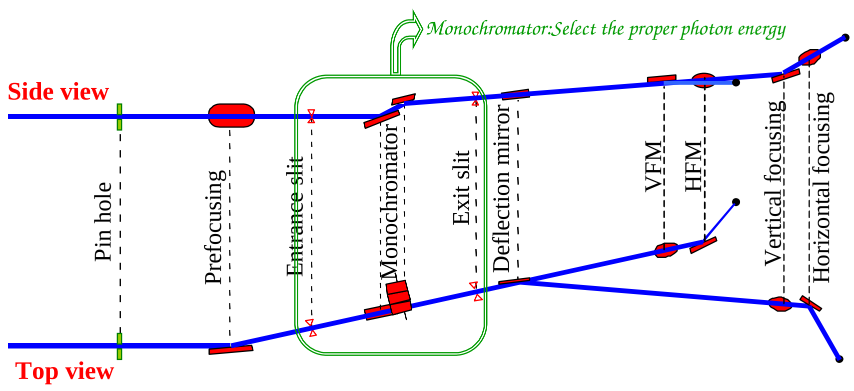

Diffraction grating

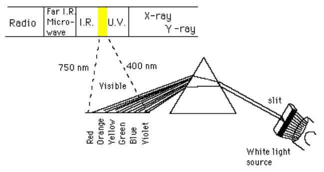

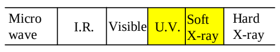

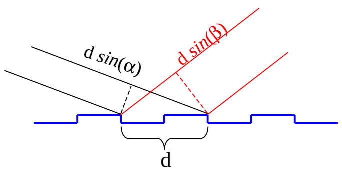

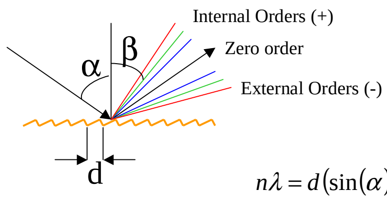

$$n\lambda = d(\sin(\alpha) - \sin(\beta))$$

Gratings profiles

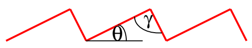

Blaze profile

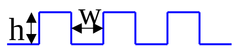

Laminar profile

Blaze gratings: *higher efficiency*

Blaze condition

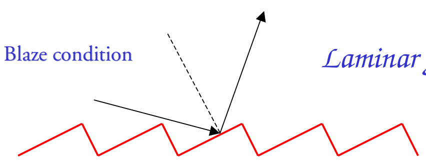

Blaze angle=(α+β)/2

Laminar gratings: *Higher spectral purity*
Higher resolution

$$n\lambda = d(\sin(\alpha) - \sin(\beta))$$

1λ, $2\frac{\lambda}{2}$

Gratings profiles

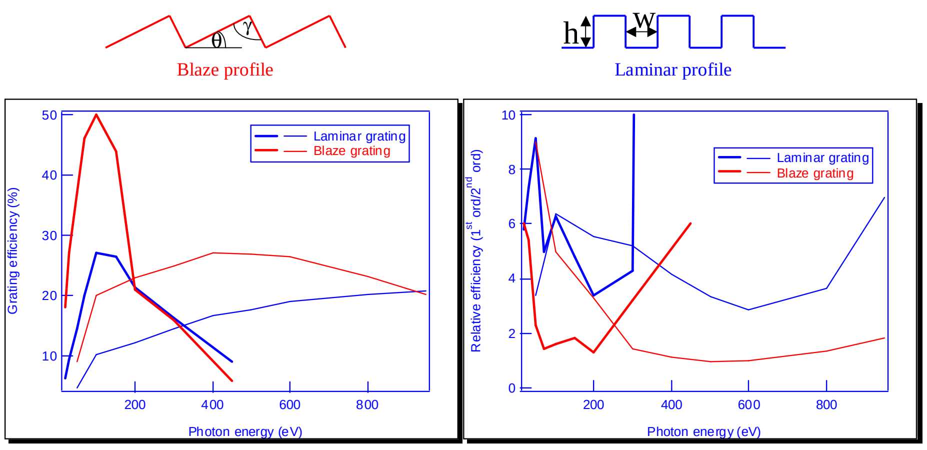

$$n\lambda = d(\sin(\alpha) - \sin(\beta))$$

the abdus salam
international centre for theoretical physics

elettra

Gratings profiles

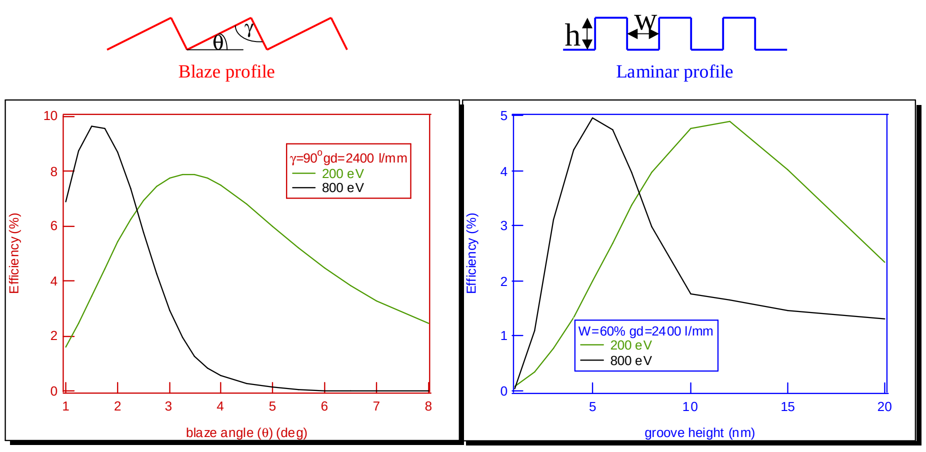

the abdus salam
international centre for theoretical physics

elettra

Diffraction grating production

Mechanical ruling *blaze profile* à *smaller blaze angles; higer efficiency*

Holographically recording *laminar and blaze profile (large blaze angle)*
à *higher groove density; lower spacing disomogeneity*

[the] abdus salam
international centre for theoretical physics

elettra

Mechanically ruled grating

Mechanically ruled (CARL ZEISS Grating Ruling Engine GTM6) with blazed profile down to 0.5-0.7°

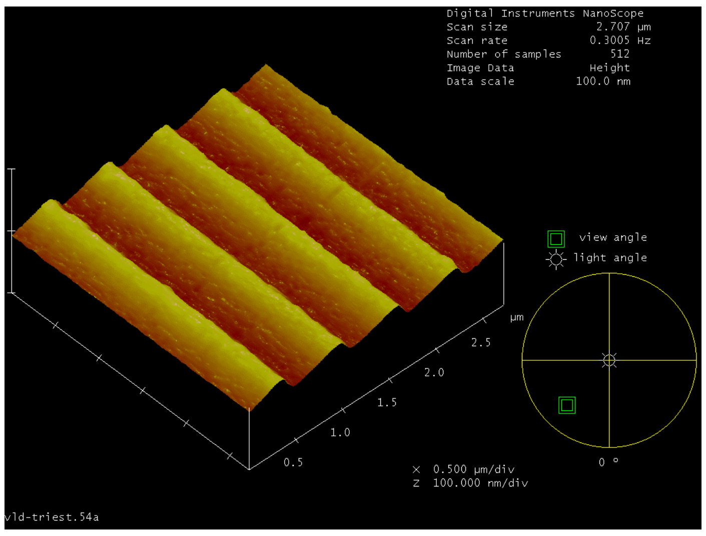

ZEISS

[the] abdus salam
international centre for theoretical physics

elettra

Holographical grating

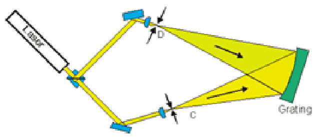

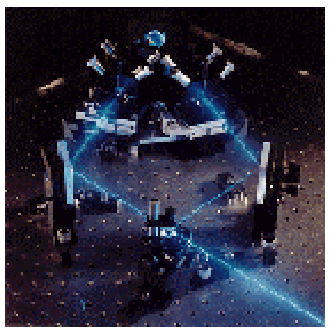

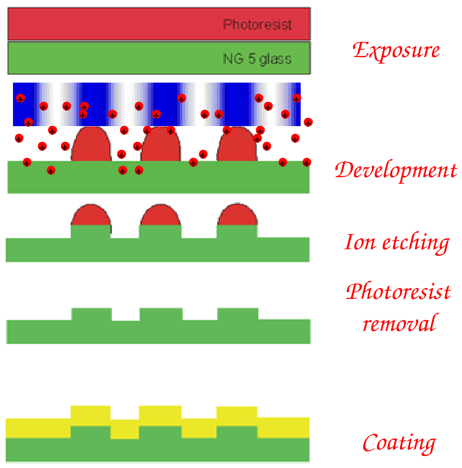

the abdus salam
international centre for theoretical physics

elettra

Holographical grating

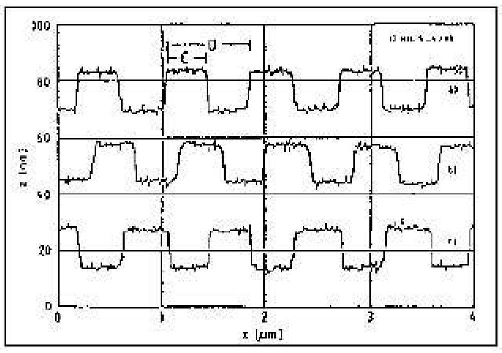

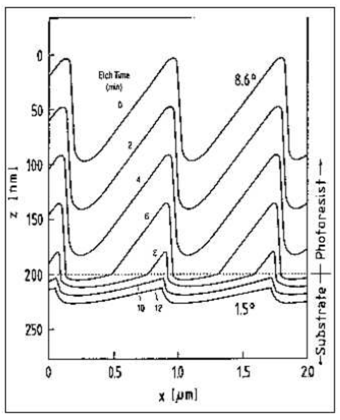

the abdus salam
international centre for theoretical physics

elettra

Gratings profiles

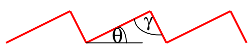

Blaze profile

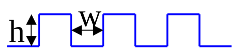

Laminar profile

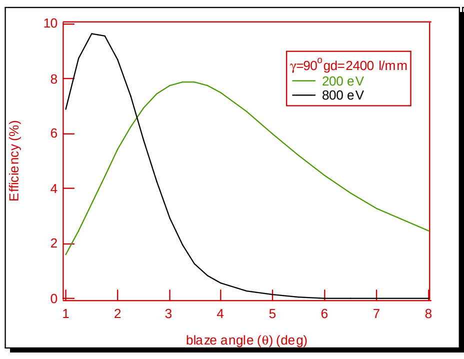

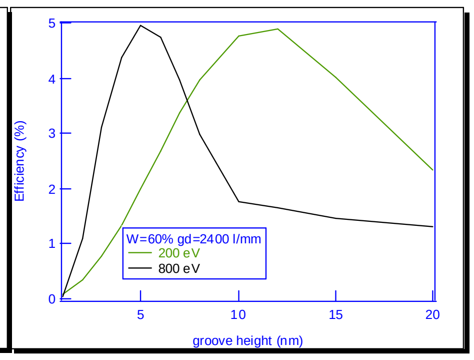

the abdus salam
international centre for theoretical physics

elettra

Shallow blaze gratings

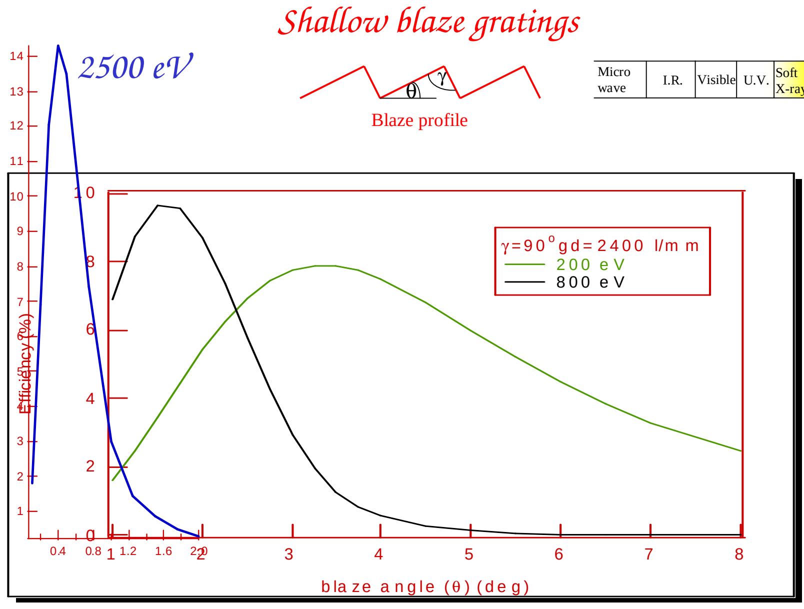

Blaze profile

Micro wave	I.R.	Visible	U.V.	Soft X-ray	Hard X-ray

the abdus salam
international centre for theoretical physics

elettra

Shallow blaze angle grating realization

ZEISS

Mechanically ruled by the CARL ZEISS Grating Ruling Engine GTM6

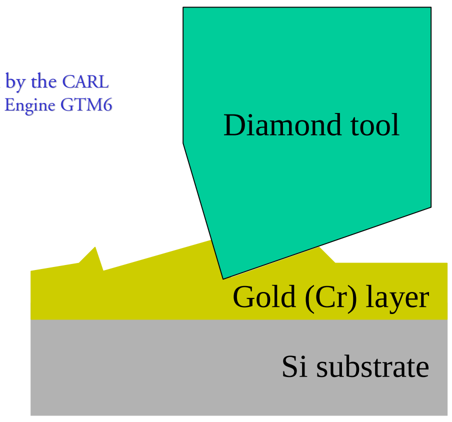

- Thermal evaporation of Gold on the Si substrate (plus Cr binding layer)
- Grooves formed by plastic deformation of the ruling layer

the abdus salam
international centre for theoretical physics

elettra

Shallow blaze angle grating realization

ZEISS

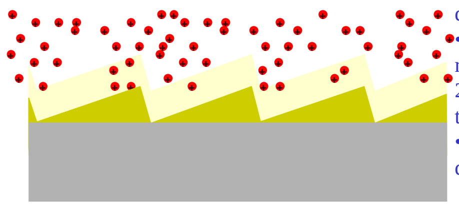

- Thermal evaporation of Gold on the Si substrate (plus Cr binding layer)
- Grooves formed by plastic deformation of the ruling layer
- Realization of low micro-roughness blaze grating with 20<gd<5000 l/mm and down to 1.5º of blaze angle
- Ar+ ion etching (200 mm diameter collimated beam)

the abdus salam
international centre for theoretical physics

elettra

Shallow blaze angle grating realization

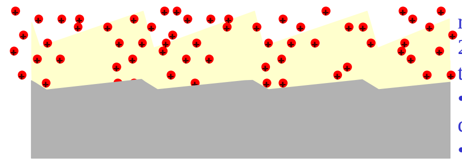

- Thermal evaporation of Gold on the Si substrate (plus Cr binding layer)
- Grooves formed by plastic deformation of the ruling layer
- Realization of low micro-roughness blaze grating with 20<gd<5000 l/mm and down to 1.5º of blaze angle
- Ar^{+} ion etching (200 mm diameter collimated beam)
- Ar^{+} ion etching rate on gold much larger then on Silicon
- An angle reduction of a factor 3 (even higher if Ar^{+} + O^{+} is used) can be achieved by this technique
- Roughness and anti blaze angle are also reduced.

Our grating

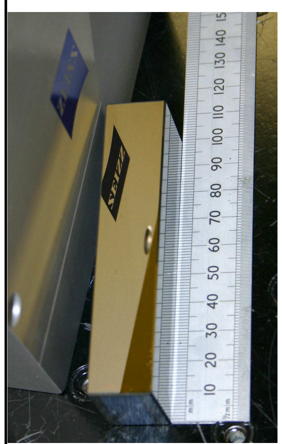

Plane substrate 600 l/mm gold coated
80X5 mm useful area, blaze angle 0.4º

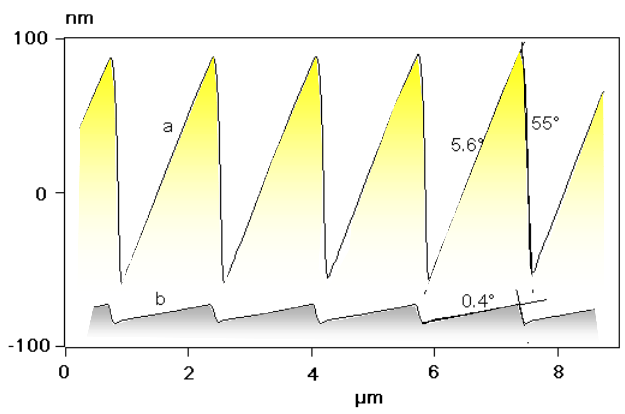

the abdus salam
international centre for theoretical physics

Expected performance

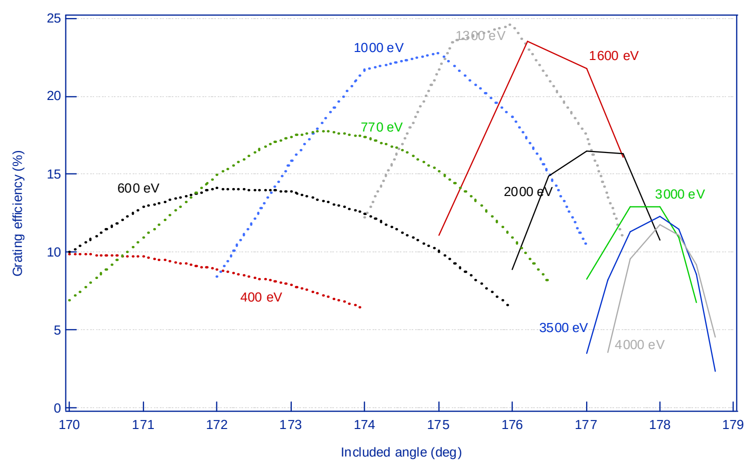

Grating's equations

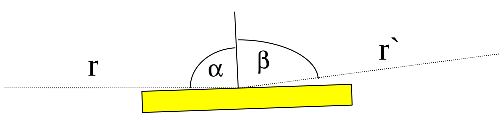

Optical path function

$$F_{100} = -n\lambda D_0 + (\sin\alpha - \sin\beta)$$ *grating equation*

$$F_{200} = \left(\frac{\cos^2\alpha}{r} - \frac{\cos\alpha}{R} + \frac{\cos^2\beta}{r'} - \frac{\cos\beta}{R}\right)$$ *tangential focus*

$$F_{300} = \left[\left(\frac{\cos^2\alpha}{r} - \frac{\cos\alpha}{R}\right)\frac{\sin\alpha}{r} + \left(\frac{\cos^2\beta}{r'} - \frac{\cos\beta}{R}\right)\frac{\sin\beta}{r'}\right]$$ *primary coma*

Rowland condition

$\mathcal{F}_{200} = \mathcal{F}_{300} = 0$

$r = R\cos\alpha$

$r' = R\cos\beta$

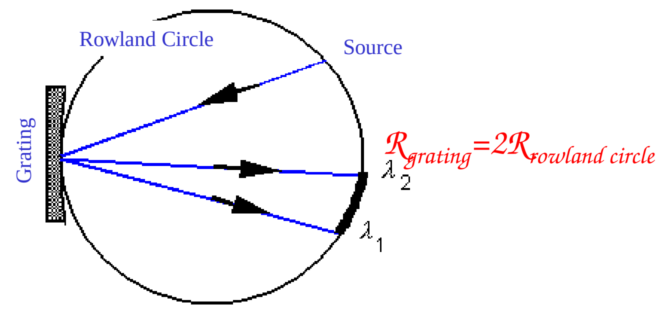

$$F_{200} = \left(\frac{\cos^2\alpha}{r} - \frac{\cos\alpha}{R}\right) + \left(\frac{\cos^2\beta}{r'} - \frac{\cos\beta}{R}\right)$$ *tangential focus*

$$F_{300} = \left[\left(\frac{\cos^2\alpha}{r} - \frac{\cos\alpha}{R}\right)\frac{\sin\alpha}{r} + \left(\frac{\cos^2\beta}{r'} - \frac{\cos\beta}{R}\right)\frac{\sin\beta}{r'}\right]$$ *primary coma*

Plane/spherical grating monochromators

$$F_{100} = -n\lambda D_0 + (\sin\alpha - \sin\beta)$$

$$F_{200} = \left(\frac{\cos^2\alpha}{r} - \frac{\cos\alpha}{R} + \frac{\cos^2\beta}{r'} - \frac{\cos\beta}{R}\right)$$

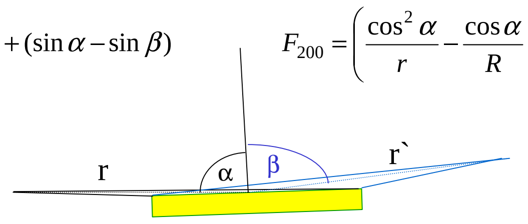

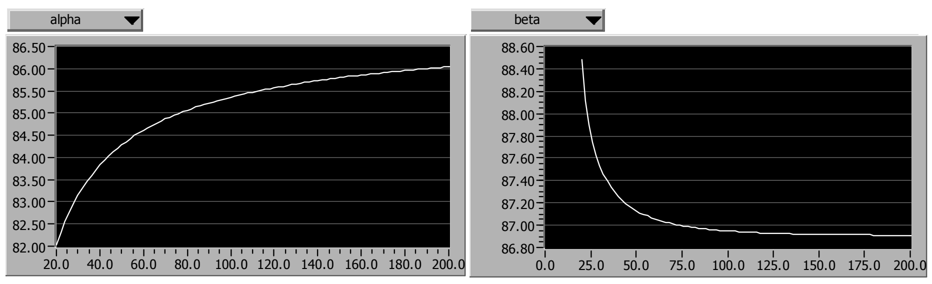

Plane/spherical grating monochromators

$$F_{100} = -n\lambda D_0 + (\sin\alpha - \sin\beta) \qquad F_{200} = \left(\frac{\cos^2\alpha}{r} - \frac{\cos\alpha}{R} + \frac{\cos^2\beta}{r'} - \frac{\cos\beta}{R}\right)$$

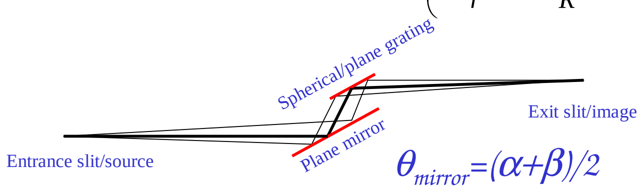

$$\theta_{mirror} = (\alpha+\beta)/2$$

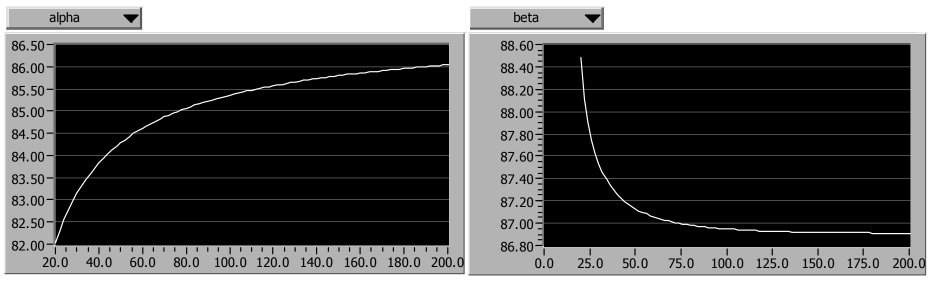

Plane/spherical grating monochromators

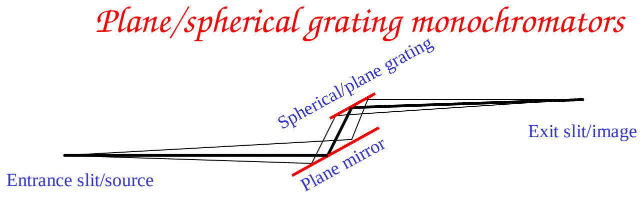

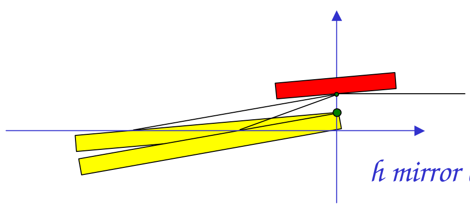

h mirror axis ~ h/2 grating center

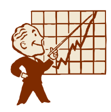

the abdus salam
international centre for theoretical physics

Plane/spherical grating monochromators

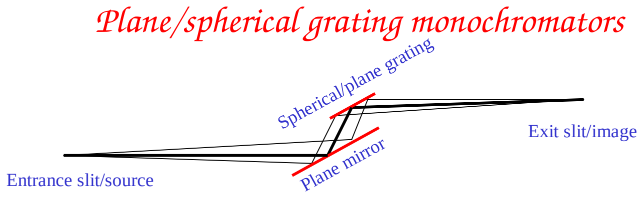

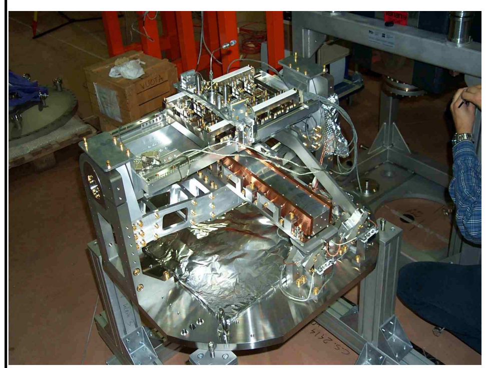

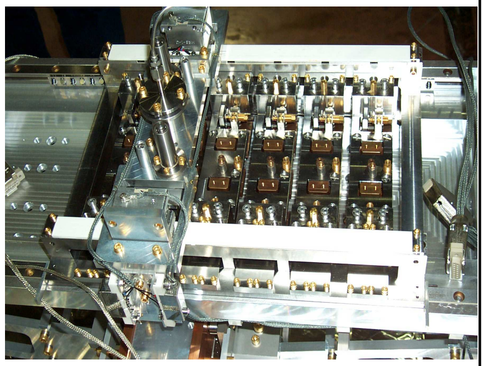

Spherical grating monochromator efficiency

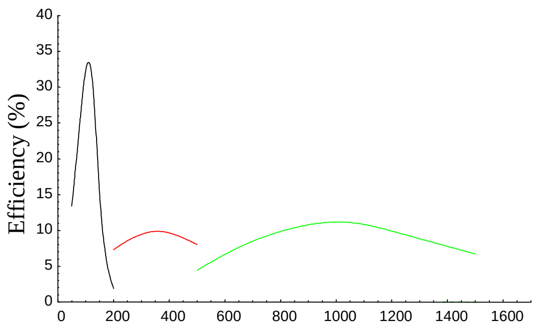

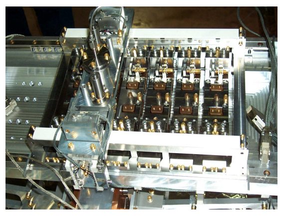

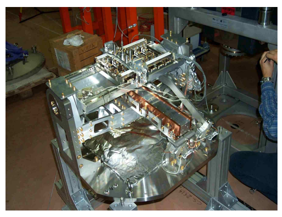

Resolving power

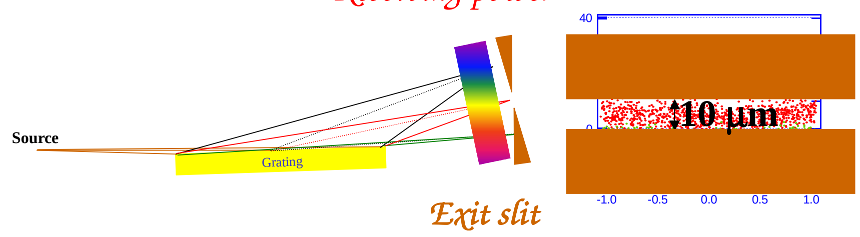

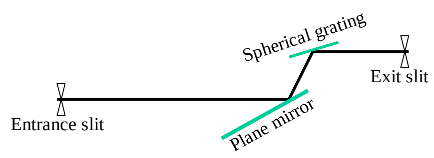

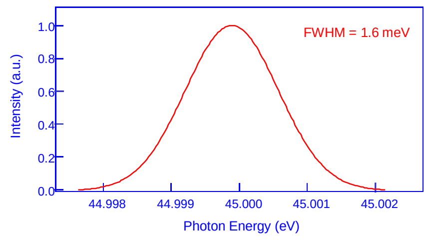

the abdus salam
international centre for theoretical physics

elettra

Resolving power

smaller are s and s´,
smaller will be the bandpass

$$Nk\lambda = \sin(\alpha) - \sin(\beta)$$

$$\left(\frac{\partial\lambda}{\partial\alpha}\right) = \frac{\cos(\alpha)}{Nk} \qquad \Delta\alpha = \frac{s}{r} \qquad \Delta\lambda_{entrance} = \frac{s\cdot\cos(\alpha)}{Nkr}$$

entrance slit contribution

$$\left(\frac{\partial\lambda}{\partial\beta}\right) = \frac{\cos(\beta)}{Nk} \qquad \Delta\beta = \frac{s'}{r'} \qquad \Delta\lambda_{exit} = \frac{s'\cdot\cos(\beta)}{Nkr'}$$

exit slit contribution

Resolving power = $E/\Delta E$

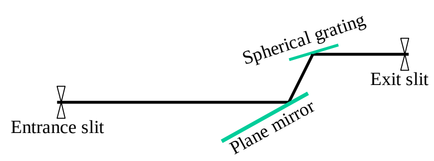

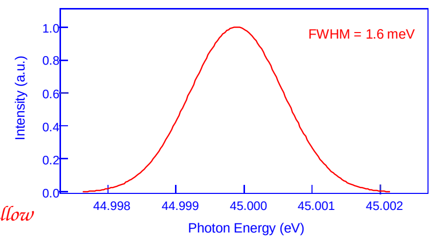

Note: the angular precision of the grating rotation have to allow the energy selection i.e. 0.2-0.3 µrad

45/0.0016 ≈ 28000

the abdus salam
international centre for theoretical physics

elettra

Resolving power

Typical Spherical grating monochromator resolving power

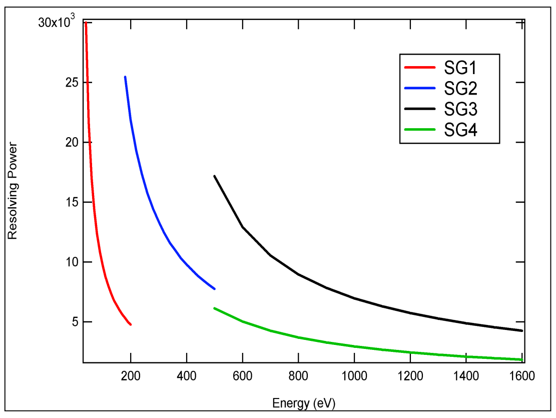

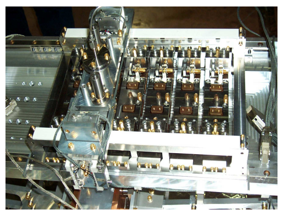

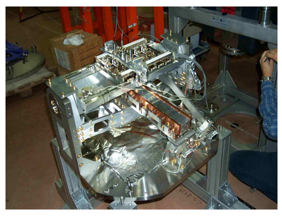

Resolving power

Typical Spherical grating monochromator resolving power

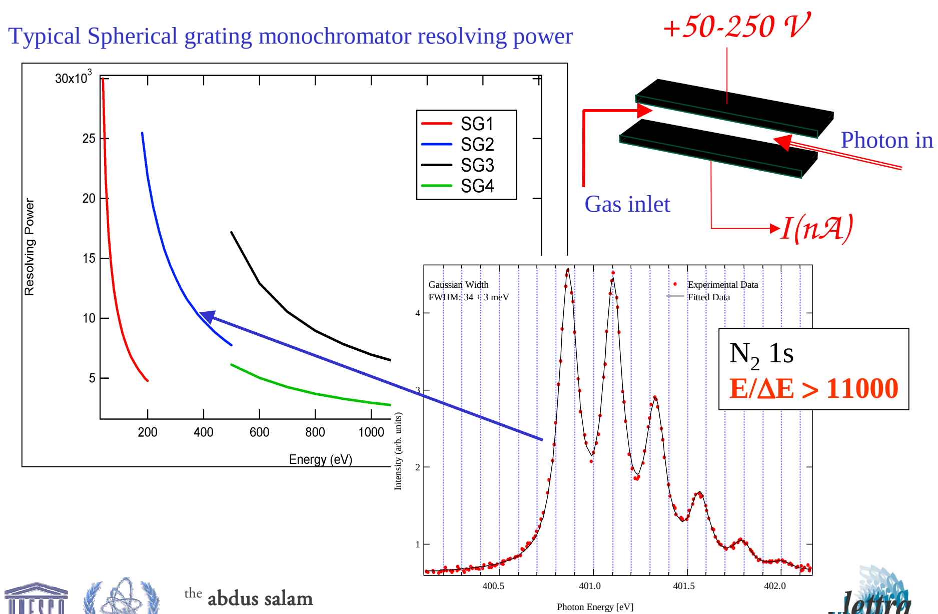

Resolving power

Typical Spherical grating monochromator resolving power

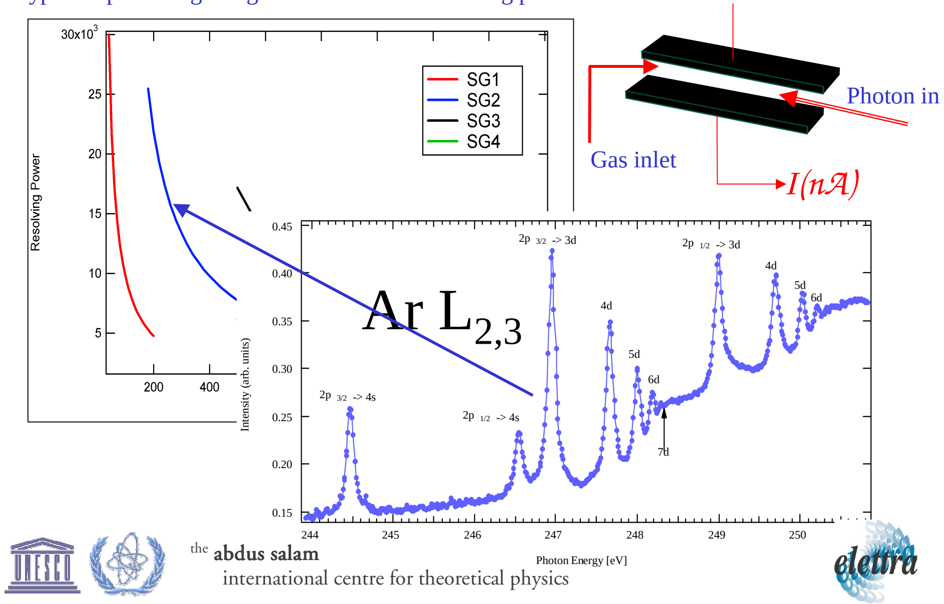

the abdus salam
international centre for theoretical physics

Resolving power

Typical Spherical grating monochromator resolving power

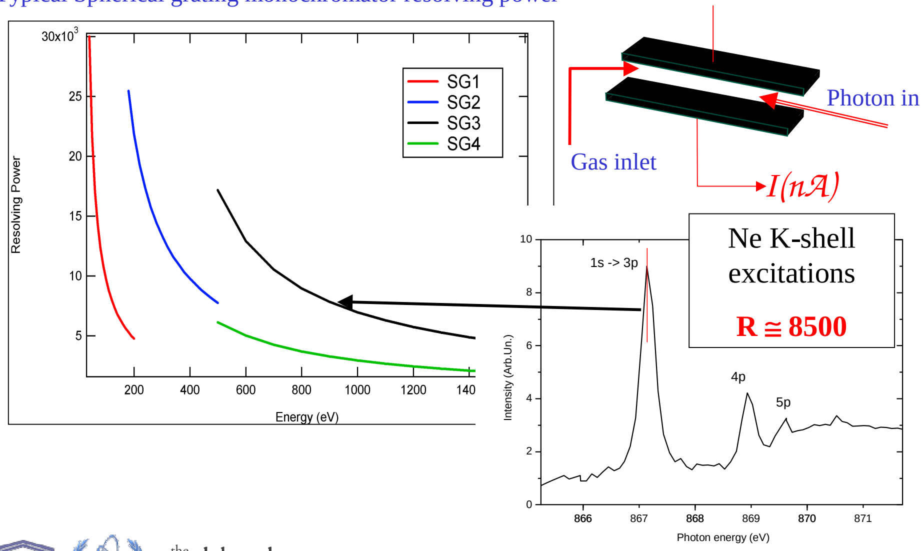

the abdus salam
international centre for theoretical physics

Resolving power

Typical Spherical grating monochromator resolving power

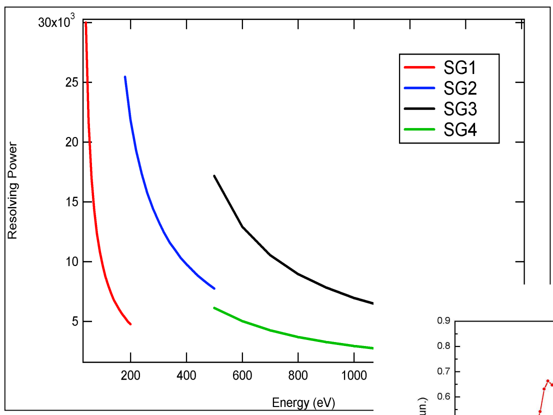

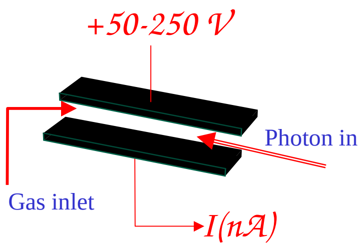

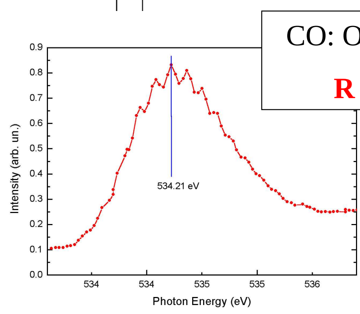

CO: O 1s $\rightarrow$ Π^*

R ≅ 8000

Magnification

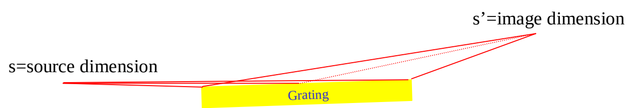

$$M(\lambda) = \frac{s'}{s}$$

$$Nk\lambda = \sin(\alpha) - \sin(\beta)$$

$$\left(\frac{\partial\lambda}{\partial\alpha}\right) = \frac{\cos(\alpha)}{Nk} \qquad \Delta\alpha = \frac{s}{r}$$

$$\left(\frac{\partial\lambda}{\partial\beta}\right) = \frac{\cos(\beta)}{Nk} \qquad \Delta\beta = \frac{s'}{r'}$$

$$M(\lambda) = \frac{s'}{s} = \frac{r'}{r}\frac{\cos(\alpha)}{\cos(\beta)}$$

Groove errors

Ghosts & Stray Light

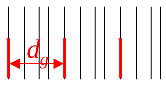

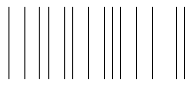

Periodic imperfections

$$\sin\beta = \sin\alpha - \frac{n\lambda}{d}$$

$$\sin\beta_g = \sin\alpha - \frac{n\lambda}{d_g}$$

$$I_g = I_0\left(\frac{n\pi\ \delta d}{d}\right)^2$$

Random imperfections

$$I = I_0 \exp-\left(\frac{2\pi\ \sin\beta\ \delta d}{\lambda}\right)$$

δd

Maximum deviation from the ideal d-spacing

rms deviation from the ideal d-spacing

Variable line space grating

Groove density D varies along the grating surface: $\mathcal{D}(x) = \mathcal{D}_0 + \mathcal{D}_1 x + \mathcal{D}_2 x^2 + \mathcal{D}_3 x^3 + \cdots$

$$\mathcal{F}_{200} = \frac{1}{2}\left(-n\lambda\mathcal{D}_1 + \left(\frac{\cos^2\alpha}{r} - \frac{\cos\alpha}{\mathcal{R}} + \frac{\cos^2\beta}{r'} - \frac{\cos\beta}{\mathcal{R}}\right)\right)$$

$$\mathcal{F}_{300} = -\frac{1}{3}n\lambda\,\mathcal{D}_2 + \frac{1}{2}\left[\left(\frac{\cos^2\alpha}{r} - \frac{\cos\alpha}{\mathcal{R}}\right)\frac{\sin\alpha}{r} + \left(\frac{\cos^2\beta}{r'} - \frac{\cos\beta}{\mathcal{R}}\right)\frac{\sin\beta}{r'}\right]$$

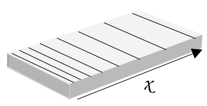

$$\mathcal{F}_{M00} = -c_M n\lambda\,\mathcal{D}_M + \mathcal{K}_{M00}$$

Reduction of higher order aberrations

Increasing of focusing property of spherical gratings

Focusing plane gratings

Constant demagnification ratio of plane VLS monochromators

Spherical Variable line space grating

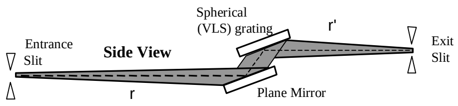

$$\mathcal{F}_{300} = -\frac{1}{3} n\lambda\, \mathcal{D}_2 + \frac{1}{2}\left[\left(\frac{\cos^2\alpha}{r} - \frac{\cos\alpha}{\mathcal{R}}\right)\frac{\sin\alpha}{r} + \left(\frac{\cos^2\beta}{r'} - \frac{\cos\beta}{\mathcal{R}}\right)\frac{\sin\beta}{r'}\right]$$

200eV

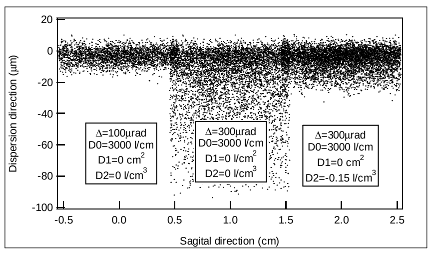

70eV

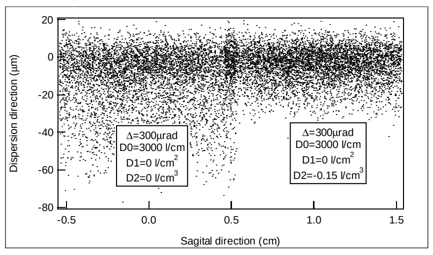

Variable line space grating

Groove density D varies along the grating surface: $\mathcal{D}(x) = \mathcal{D}_0 + \mathcal{D}_1 x + \mathcal{D}_2 x^2 + \mathcal{D}_3 x^3 + \cdots$

$$\mathcal{F}_{200} = \frac{1}{2}\left(-n\lambda\mathcal{D}_1 + \left(\frac{\cos^2\alpha}{r} - \frac{\cos\alpha}{\mathcal{R}} + \frac{\cos^2\beta}{r'} - \frac{\cos\beta}{\mathcal{R}}\right)\right)$$

$$\mathcal{F}_{300} = -\frac{1}{3} n\lambda\, \mathcal{D}_2 + \frac{1}{2}\left[\left(\frac{\cos^2\alpha}{r} - \frac{\cos\alpha}{\mathcal{R}}\right)\frac{\sin\alpha}{r} + \left(\frac{\cos^2\beta}{r'} - \frac{\cos\beta}{\mathcal{R}}\right)\frac{\sin\beta}{r'}\right]$$

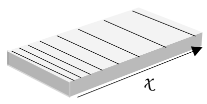

$$\mathcal{F}_{M00} = -c_M n\lambda\, \mathcal{D}_M + \mathcal{K}_{M00}$$

Reduction of higher order aberrations

Increasing of focusing property of spherical gratings

Focusing plane gratings

Constant demagnification ratio of plane VLS monochromators

Spherical VLS spectrometer (ComIXS)

Groove density D varies along the grating surface: $\mathcal{D}(x)=\mathcal{D}_0+\mathcal{D}_1 x+\mathcal{D}_2 x^2+\mathcal{D}_3 x^3+\cdots$

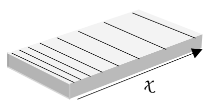

$$\mathcal{F}_{200}=\frac{1}{2}\left(-n\lambda\mathcal{D}_1+\left(\cancel{\frac{\cos^2\alpha}{r}-\frac{\cos\alpha}{\mathcal{R}}}+\frac{\cos^2\beta}{r'}-\frac{\cos\beta}{\mathcal{R}}\right)\right)$$

$$\mathcal{F}_{300}=-\frac{1}{3}n\lambda\,\mathcal{D}_2+\frac{1}{2}\left[\cancel{\left(\frac{\cos^2\alpha}{r}-\frac{\cos\alpha}{\mathcal{R}}\right)}\frac{\sin\alpha}{r}+\left(\frac{\cos^2\beta}{r'}-\frac{\cos\beta}{\mathcal{R}}\right)\frac{\sin\beta}{r'}\right]$$

If distance source-grating and angle of incidence are kept constant i.e. $\mathcal{R}=\frac{r}{\cos\alpha}$

$$\mathcal{F}_{200}=\frac{1}{2}\left(-n\lambda\mathcal{D}_1+\left(\frac{\cos^2\beta}{r'}-\frac{\cos\beta}{\mathcal{R}}\right)\right)=0 \Longrightarrow r'=f\left(\beta(\lambda),\mathcal{D}_1\right)$$

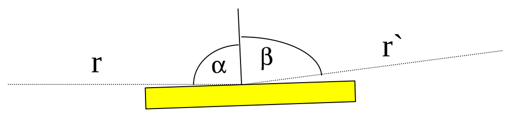

Spherical VLS spectrometer (ComIXS)

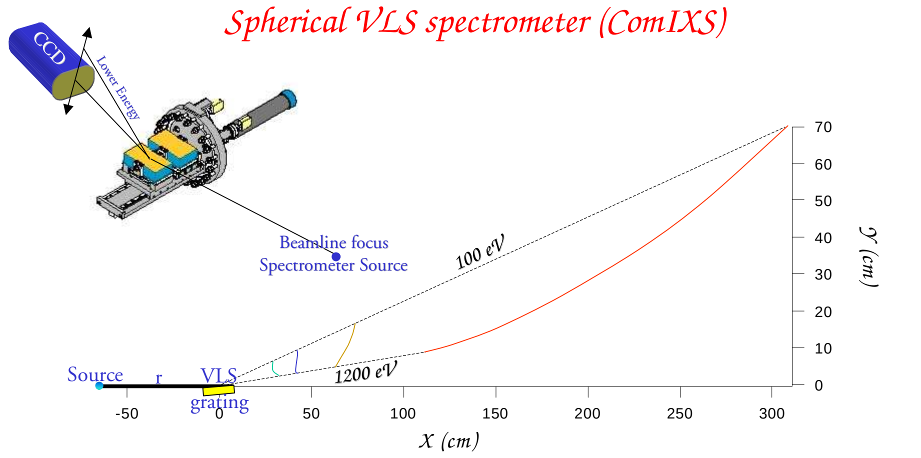

D_1=0 **D_1=400 l/cm²** **D_1=800 l/cm²** **D_1=1200 l/cm²**

$$\mathcal{F}_{200}=\frac{1}{2}\left(-n\lambda\mathcal{D}_1+\left(\frac{\cos^2\beta}{r'}-\frac{\cos\beta}{\mathcal{R}}\right)\right)$$

D_0=19200 l/cm
r=63 cm
R≈14 m

the abdus salam
international centre for theoretical physics
elettra

Compact Inelastic X-ray spectrometer

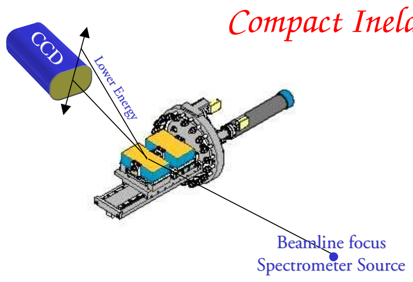

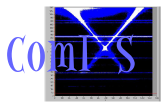

Distance sample grating (cm)	63	
Distance grating CCD (cm)	*variable* ≈ 42	
Angle of incidence(deg)	87.48	
radius of curvature (cm)	1432.7	
	LEG	HEG
Energy range (eV)	**25-200**	**100-1200**
D_0 (l/cm)	**4800**	**19200**
D_1 (l/cm^2)	**200**	**800**
D_2 (l/cm^3)	**7.5**	**30**

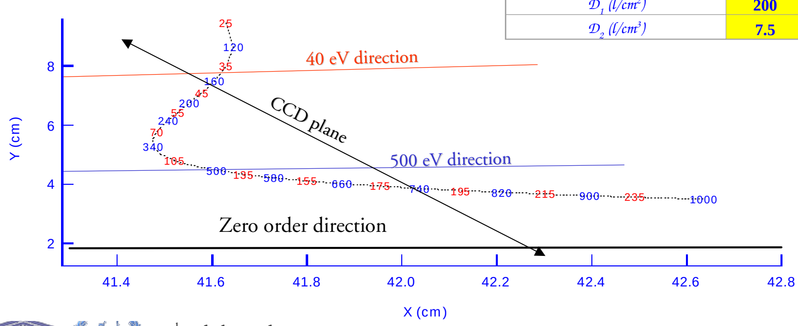

the **abdus salam** international centre for theoretical physics

elettra

Plane VLS grating

Groove density D varies along the grating surface: $\mathcal{D}(x) = \mathcal{D}_0 + \mathcal{D}_1 x + \mathcal{D}_2 x^2 + \mathcal{D}_3 x^3 + \cdots$

$$\mathcal{F}_{200} = \frac{1}{2}\left(-n\lambda\mathcal{D}_1 + \left(\frac{\cos^2\alpha}{r} - \frac{\cos\alpha}{\mathcal{R}} + \frac{\cos^2\beta}{r'} - \frac{\cos\beta}{\mathcal{R}}\right)\right)$$

$$\mathcal{F}_{300} = -\frac{1}{3}n\lambda\,\mathcal{D}_2 + \frac{1}{2}\left[\left(\frac{\cos^2\alpha}{r} - \frac{\cos\alpha}{\mathcal{R}}\right)\frac{\sin\alpha}{r} + \left(\frac{\cos^2\beta}{r'} - \frac{\cos\beta}{\mathcal{R}}\right)\frac{\sin\beta}{r'}\right]$$

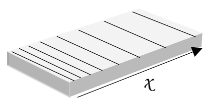

$$\mathcal{F}_{200} = \frac{1}{2}\left(-n\lambda\mathcal{D}_1 + \left(\frac{\cos^2\alpha}{r} + \frac{\cos^2\beta}{r'}\right)\right)$$ *A plane grating can focus!*

$$\mathcal{F}_{300} = -\frac{1}{3}n\lambda\,\mathcal{D}_2 + \frac{1}{2}\left[\frac{\sin\alpha\cos^2\alpha}{r^2} + \frac{\sin\beta\cos^2\beta}{r'^2}\right]$$

$$F_{100} = -n\lambda D + (\sin\alpha - \sin\beta)$$

$$\sin\beta = \sin\alpha - n\lambda D$$

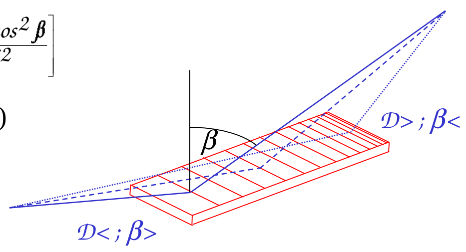

the **abdus salam** international centre for theoretical physics

elettra

Plane VLS grating (nanospectroscopy)

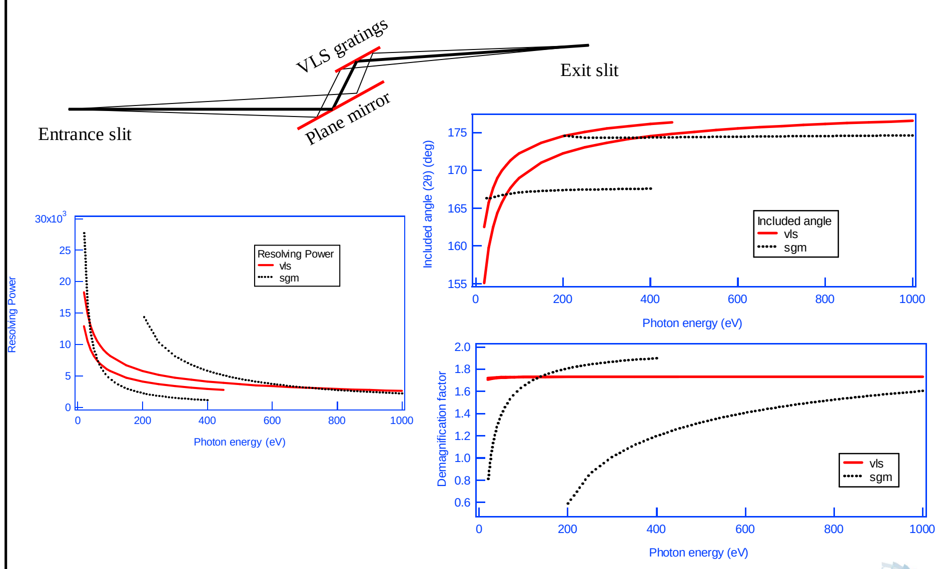

Microfocusing

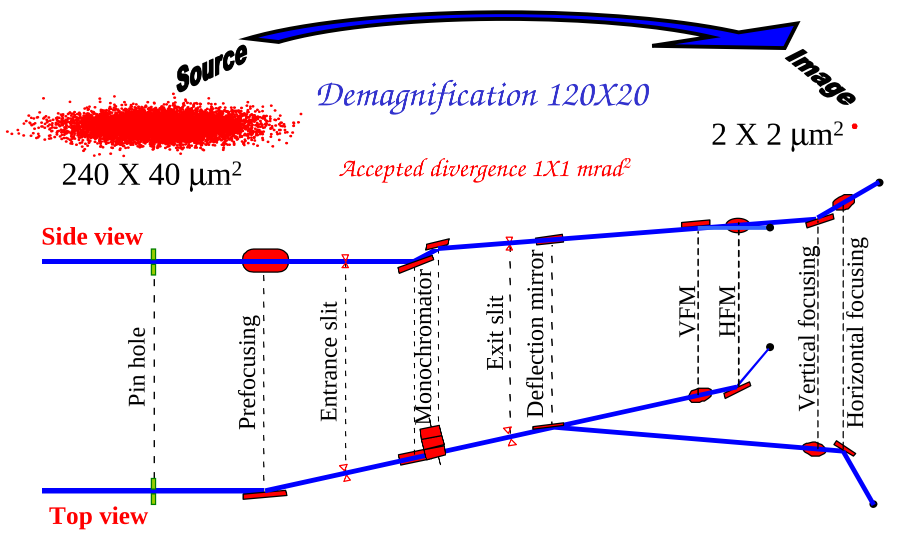

Kirkpatrick Baez configuration

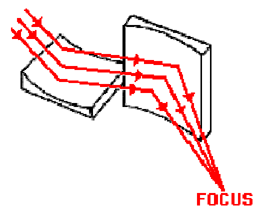

$$(1/r+1/r')\cos\theta/2=1/R$$

Microfocusing

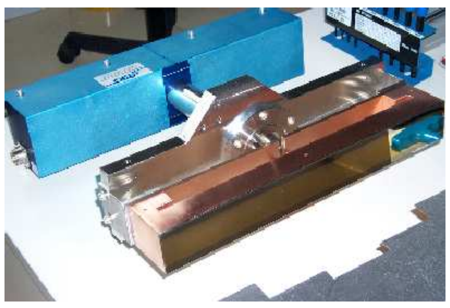

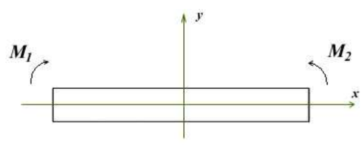

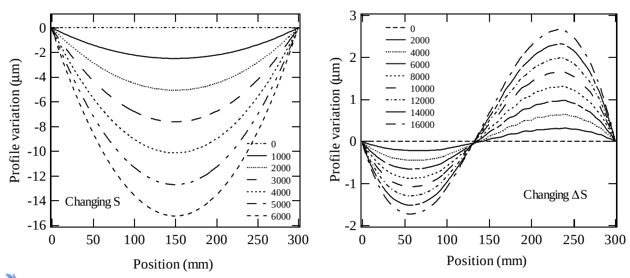

Microfocusing

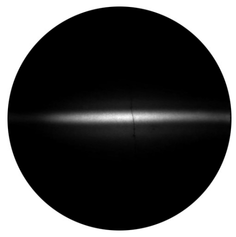

Sample tilted by 76°

$2X7\ \mu m^2$
Flux $1x10^{13}$ ph/sec

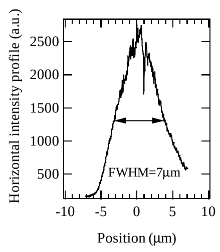

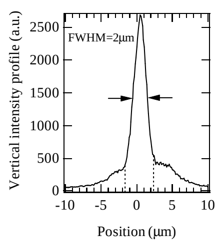

Mechanical bender (ESRF)

micro-fluorescence & micro-diffraction (HXR)

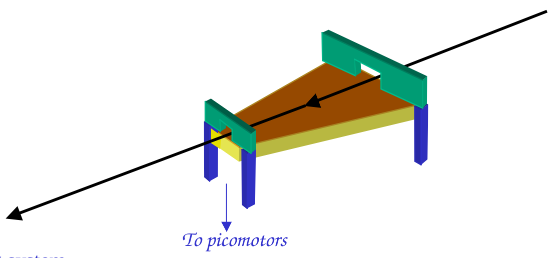

Bending system

The mirror must be shaped according to the required working distance and angle of incidence constant thickness but linear width variation.

Open clamping system to let the beam pass trough

Picomotors for the bending driving system (2 for each mirror)
Two different moments are applied at the end of the flat polished substrate

the abdus salam
international centre for theoretical physics
elettra

Mechanical bender (ESRF)

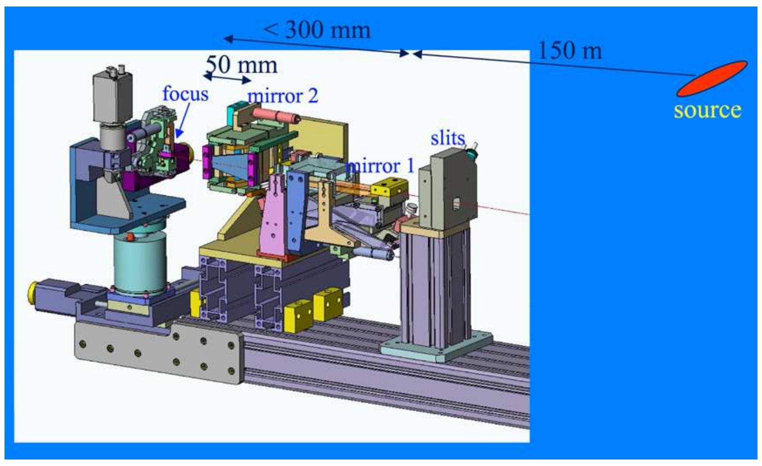

Homogeneous spot

elettra

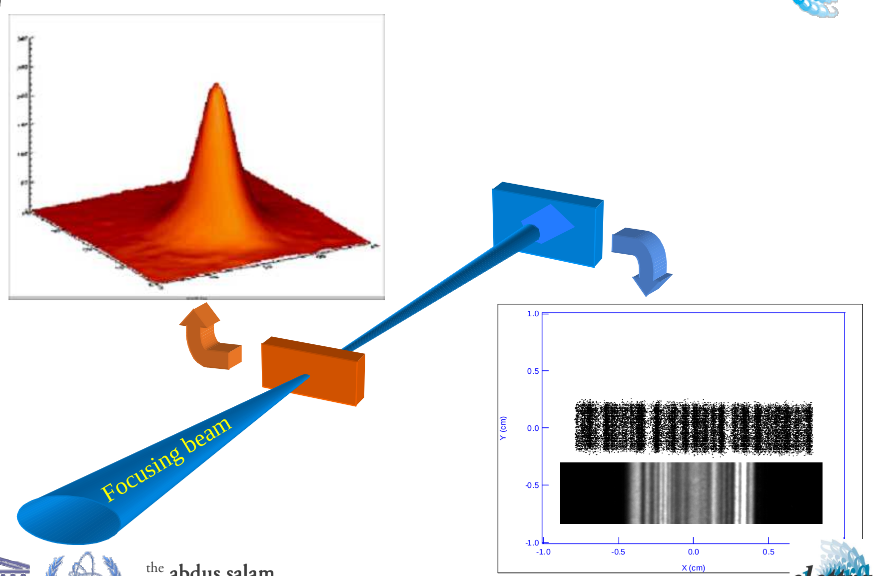

the abdus salam
international centre for theoretical physics

elettra

EUV and soft x-ray optics

Homogeneous spot

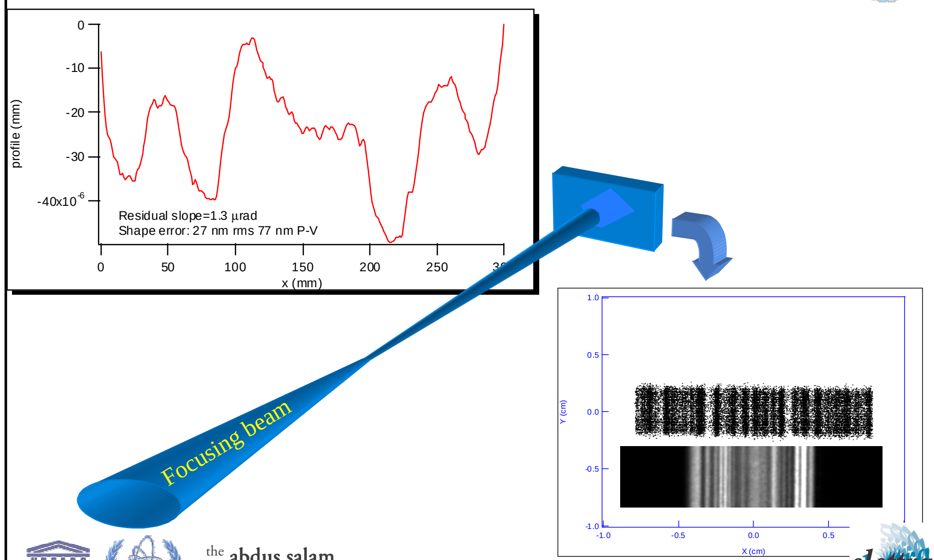

Piezoelectric Bimorph mirrors

R. Signorato (ACCEL)
J.J. Fermé S.E.S.O.

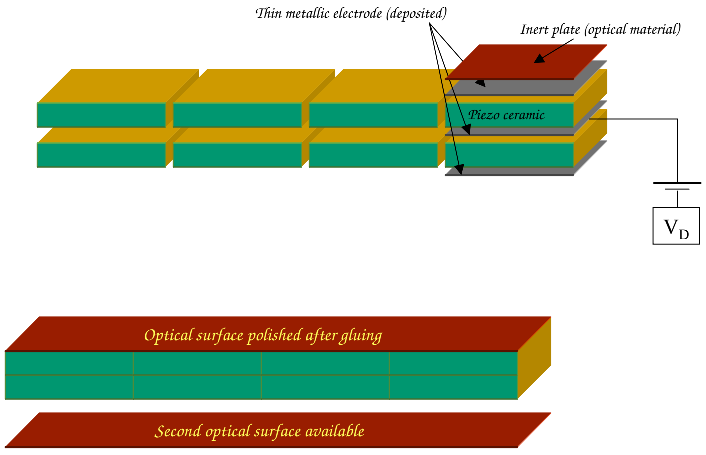

Piezoelectric Bimorph mirrors

Dimension: from 150 mm (single element) to 1400 mm.

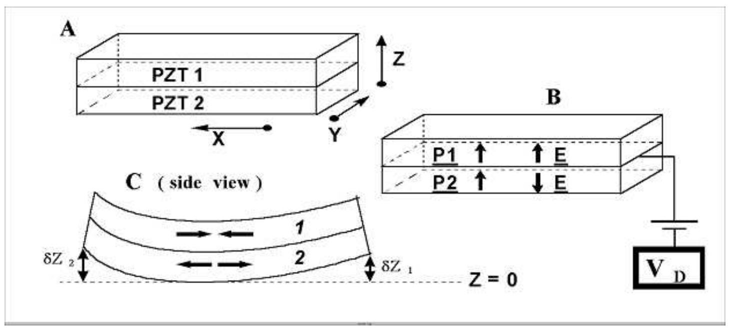

Radius variation: 370 m (+1500V) to 2300 m (-1500V)

Stability: $\Delta R/R \cong 0.8\%$ on 1 day scale
$\Delta R/R \cong 2.0\%$ on 10 day scale

Metrology

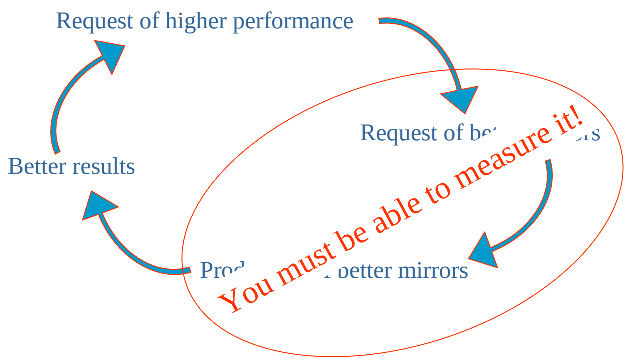

the abdus salam
international centre for theoretical physics
elettra

Metrology laboratory

Clean room class 1000 (BIOAIR) | **Thermostabilised room** ($\Delta T = 0.1^{o}$ rms)

Micromap Promap 512 Reichert POLIVAR 2 MET	WYKO RTI 4100	Long trace profiler (LTP II)
	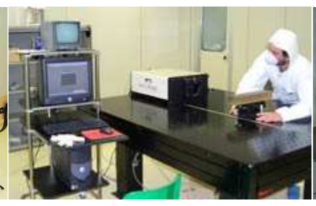	
Purchased in 1992 *Roughness measurement* *Good repeatability and precision (better then 1Å rms)*	*Purchased in 2002* *3D surface topography*	*Purchased in 1991* *Several in house modification* *2D direct slope measurement*

Long trace profiler (LTP)

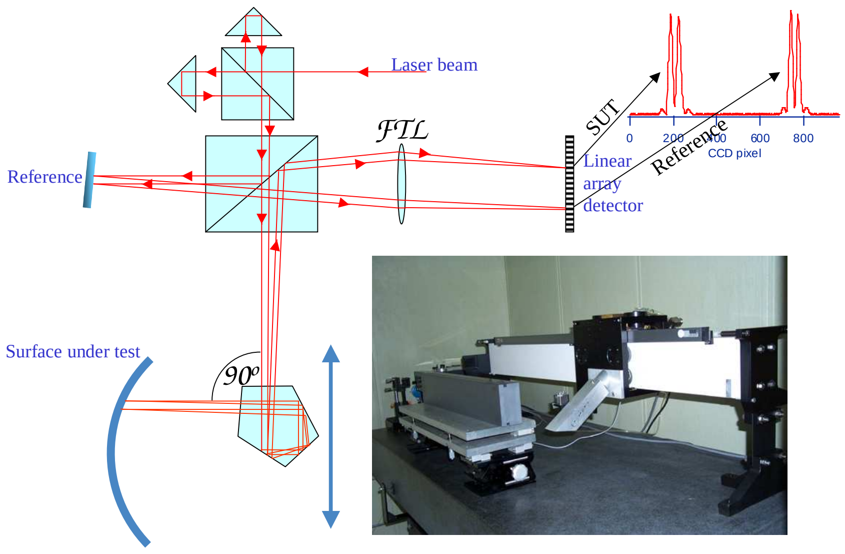

Long trace profiler (LTP)

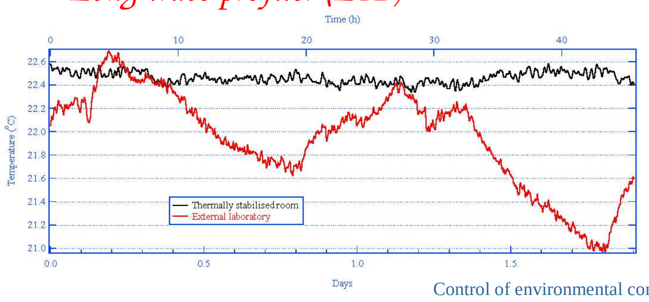

Control of environmental conditions
-Thermalisation of the laboratory
-Absence of air turbulence
-Remote control measurement
-Stable supports

the abdus salam
international centre for theoretical physics

elettra

Groove density measurement

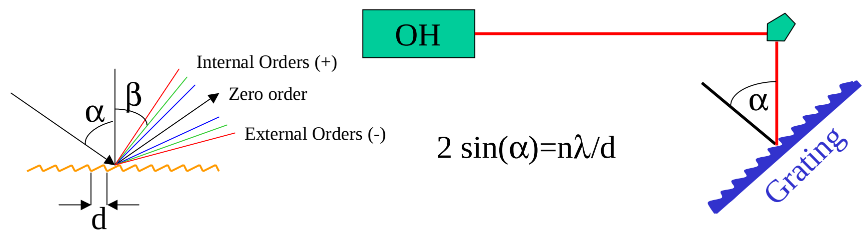

$2\sin(\alpha)=n\lambda/d$

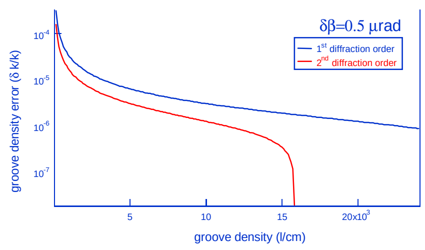

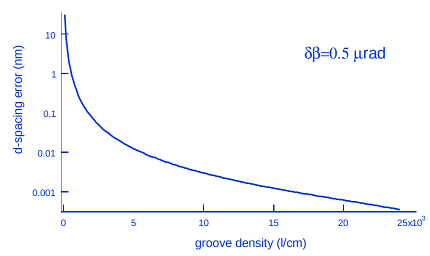

the abdus salam
international centre for theoretical physics

elettra

WYKO RTI 4100

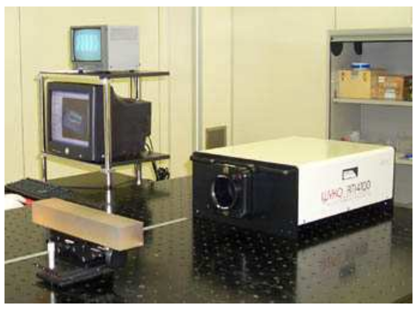

3D measurement of optical surfaces

λ/100 precision
λ/2000 repeatability

Accessories
Transmission spheres
f /1.5 for sagittal radii and NI mirrors with R<1 m
f /24.8 diverger for NI mirrors with R>2 m

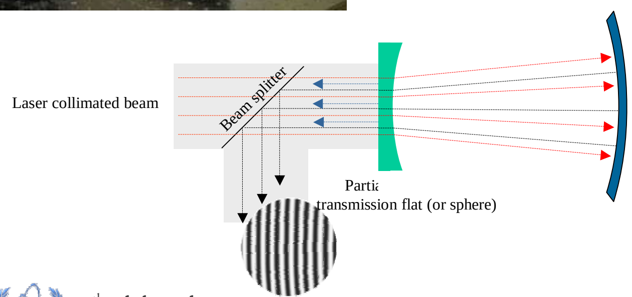

the abdus salam
international centre for theoretical physics

elettra

Roughness measurment (Micromap Promap)

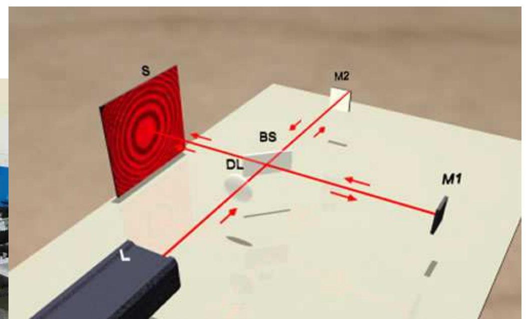

Precision 0.5 Å rms
Spatial frequency:
1 μm^{-1} to 1 mm^{-1}

the abdus salam
international centre for theoretical physics

elettra

AFM measurement

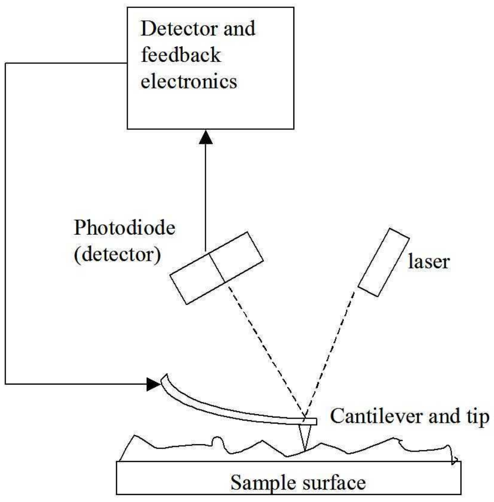

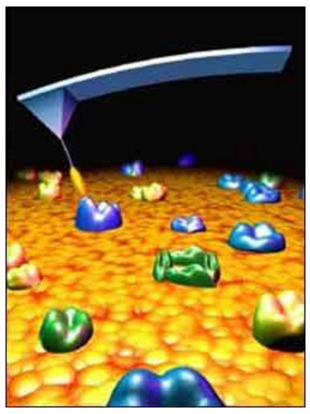

the abdus salam
international centre for theoretical physics

AFM measurement

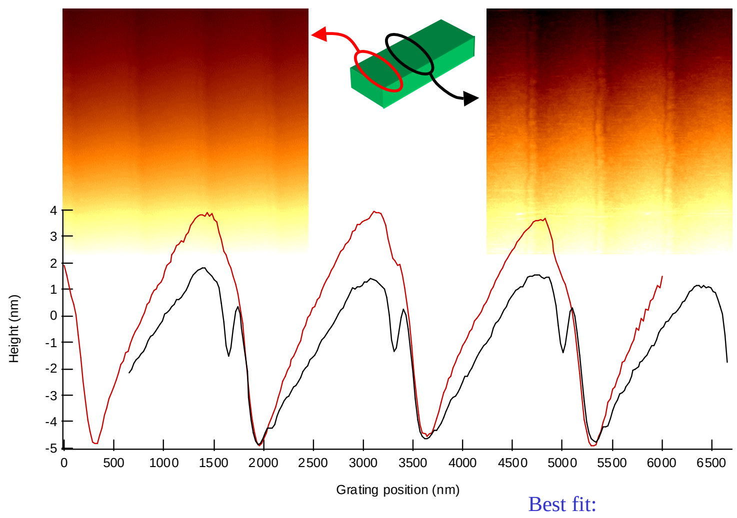

Best fit:
blaze=0.4° antibleze=1.34°

the abdus salam
international centre for theoretical physics